The Security-Reliability Tradeoff of Multiuser Scheduling Aided Energy Harvesting Cognitive Radio Networks

Xiaojin Ding*†, Yulong Zou, *Senior Member, IEEE,* Genxin Zhang, *Member, IEEE,* Xiaoshu Chen, Xiaojun Wang and Lajos Hanzo, *Fellow, IEEE*

***Abstract*—We study the physical-layer security of a cognitive radio system in the face of multiple eavesdroppers (EDs), which is composed of a secondary base station (SBS), multiple secondary users (SUs) as well as a pair of primary transmitter (PT) and primary receiver (PR), where the SUs first harvest energy from their received radio frequency signals transmitted by the PT and then communicate with the SBS relying on opportunistic scheduling. We consider two specific user scheduling schemes, namely the channel-aware user scheduling (CaUS) and energy-aware user scheduling (EaUS). In the CaUS scheme, an SU having the best instantaneous SU-SBS link (spanning from SUs to SBS) will be activated to communicate with the SBS. By contrast, the EHbUS scheme takes into account both the amount of energy harvested from the PT and the instantaneous quality of the SU-SBS link. We analyze the security-reliability tradeoff (SRT) of both the CaUS and of the EaUS schemes in terms of their intercept vs outage probability. We also provide the SRT analysis of traditional round-robin user scheduling (RrUS) used as a benchmarker of the CaUS and EaUS schemes. We demonstrate that the EaUS scheme achieves the best outage and secrecy performance in the high main-to-eavesdropper ratio (MER) region, but a worse secrecy performance than the CaUS method in the low-MER region. Moreover, from a security vs reliability perspective, the CaUS outperforms both the EaUS and the RrUS in the low-MER region. Surprisingly, this also implies that although the user scheduling criterion of EaUS exploits the knowledge of both the amount of harvested power and instantaneous channel state information (CSI), it exhibits a degraded physical-layer security in the low-MER region, due to the increased harvested energy is beneficial not only for the legitimate SBS receiver, but also for the EDs.**

***Index Terms*—Cognitive radio networks, energy harvesting, user scheduling, physical-layer security, outage probability, intercept probability.**

X. Ding* is with the Jiangsu Engineering Research Center of Communication and Network Technology, Nanjing University of Posts and Telecommunications, Nanjing 210003, China. E-mail: dxj@njupt.edu.cn

Y. Zou, and G. Zhang are with the School of Telecommunications and Information Engineering, Nanjing University of Posts and Telecommunications, Nanjing 210003, China. E-mail: {yulong.zou, zgx}@njupt.edu.cn

X. Ding†, X. Chen, and X. Wang are with the National Mobile Communications Research Laboratory, Southeast University, Nanjing 210096, China. E-mail: dxj@njupt.edu.cn, {xchen, wxj}@seu.edu.cn

L. Hanzo is with the Department of Electronics and Computer Science, University of Southampton, Southampton, United Kingdom. (E-mail: lh@ecs.soton.ac.uk)

This work presented was partially supported by the National Science Foundation of China (No. 91738201 and 61671253), the China Postdoctoral Science Foundation (No. 2018M632347), the Natural Science Foundation of Jiangsu Province (No. BK20171446), the Natural Science Research of Higher Education Institutions of Jiangsu Province (No. 18KJB510030), the open research fund of National Mobile Communications Research Laboratory, Southeast University (No. 2018D16) and the Open Research Fund of Jiangsu Engineering Research Center of Communication and Network Technology, NJUPT. *(Corresponding authors are Yulong Zou, Genxin Zhang, and Lajos Hanzo)*

I. INTRODUCTION

ENERGY harvesting is capable of extracting energy from the surrounding environment, which is emerging as an efficient technique of supplying energy and has been beneficially integrated into cognitive radio (CR) systems [1,2] for extending the life-time of energy-constrained networks, whilst reducing their deployment cost. There are two widely adopted energy harvesting architectures, namely power splitting (PS) and time switching (TS) [3,4]. In a PS architecture, the received signal power can be split into two parts, where a certain fraction is used for harvesting energy, while the rest is used for processing the received signal. By contrast, in a TS architecture, the transmission slot is divided into two phases. In the first phase, the system harvests energy from the surrounding environment and the harvested energy is used for transmitting the signal in the second phase. In CR networks, the SUs are vulnerable to both internal as well as to external attacks [5]. Furthermore, due to the broadcast nature of radio propagation, the confidential messages transmitted in the CR networks may become overheard by malicious EDs. Hence, apart from maintaining the reliability of transmission, we have to protect the CR networks against malicious eavesdropping.

Physical-layer security (PLS) [6], [7] has received increasing research attention as a benefit of its ability of exploiting the physical characteristics of wireless channels to guard against wiretapping. In [8] and [9], multiple-input multiple-output (MIMO) schemes were invoked for the sake of enhancing the instantaneous secrecy rate. Beamforming techniques [10], [11] were also developed for wireless secrecy improvement. Additionally, jamming schemes [12], [13] were conceived for preventing wiretapping by the E at the expense of negligible interference imposed on the legitimate nodes, demonstrating that transmitting specifically designed artificial noise enhances the security of wireless communications. As a design alternative, both user scheduling schemes [14], [15] as well as relay selection schemes [16]-[19] were advocated for upgrading the security of wireless communications. Specifically, cooperative jamming aided user scheduling schemes have been proposed in [14] and [15], relying on a physical-layer security perspective. The authors of [16] and [17] conceived one-way relay selection schemes to assist the wireless transmissions of the source, demonstrating that the relay selection schemes are indeed capable of improving the secrecy of wireless transmissions. Moreover, two-way relay selection schemes have been proposed in [18] and [19] for physical-layer security improvement.

As a further development, PLS has also been designed for energy harvesting aided CR networks. In contrast to conventional CR networks, more efforts should be invested in enhancing the security vs reliability tradeoff of CR networks relying on both energy harvesting (EH) and PLS. The secrecy beamforming concept has been proposed in [20] for improving the physical-layer security of energy-harvesting-based CR networks. Moreover, sophisticated jamming schemes have been investigated in [21] and [22]. To be specific, in [21], a novel wireless EH cooperative jammer-aided transmission scheme was conceived for enhancing the security for cooperative CR networks. In order to improve the security of the primary network, an artificial-noise-aided cooperative jamming scheme was provided in [22] for a multiple-input single-output CR network. Furthermore, in [23], an optimal relay selection based two EH protocols has been proposed to achieve a better tradeoff between the security of primary transmission and the efficiency of secondary transmission. In [24], the authors investigated an underlay MIMO CR network consisting of a pair of primary nodes, a couple of secondary nodes as well as an E, and the secrecy outage performance of the proposed the optimal antenna selection and suboptimal antenna selection schemes have been analyzed.

Against this background, we explore the PLS of a energy harvesting oriented cognitive network comprised of multiple SUs in the presence of multiple EDs, where the SUs harvest energy from the primary transmitter at the beginning of the transmission slot. Then, in order to enhance the SRT performance, they will be chosen to communicate opportunistically with the SBS according to our user scheduling criterion. In contrast to [20]-[24], in this paper, multiple users and multiple EDs are considered. Moreover, the EDs are allowed to act cooperatively, and they are equipped with multiple antennas. Additionally, the transmit power of a SU is constrained to the minimum value between the harvested energy and the maximum tolerable interference imposed on the primary receiver. Furthermore, this paper focuses on striking a tradeoff between the security and the reliability. ***Explicitly, the main contributions of this paper are summarized as follows.***

Firstly, we present a pair of beneficial user scheduling schemes. The first one is termed as the channel-aware user scheduling (CaUS), while the second one is referred to as energy-aware user scheduling (EaUS). To be specific, in the CaUS scheme, the particular user having the maximal channel gain of the SU-SBS link will be selected as the cooperative transmission user. By contrast, the specific user having the maximal achievable rate will transmit in a given time slot of the EaUS scheme, which relies both on the channel state information (CSI) of the main links (spanning from the SUs to the SBS) and on the amount of harvested energy.

Secondly, we analyze both the outage probability (OP) and intercept probability (IP) of the CaUS and EaUS schemes for transmission over Rayleigh fading channels. We also evaluate the OP and IP of the traditional round-robin user scheduling (RrUS) scheme for comparison. Moreover, we will show that the EaUS scheme outperforms the RrUS and EaUS schemes in terms of its OP, whereas the CaUS scheme achieves a better IP than that of the EaUS scheme, indicating a tradeoff between the IP and the OP of the CaUS and EaUS schemes. It is plausible that scheduling SUs based on the amount of harvested energy in the EaUS scheme may be capable of enhancing the reliability of the wireless transmission of the SUs-SBS links, but this is also beneficial for the wiretap links (spanning from the SUs to EDs), especially if a legitimate user is activated when it has a low channel gain for the main link and simultaneously a high harvested energy.

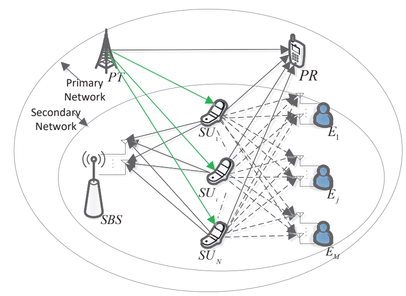

Fig. 1. Energy-harvesting aided cognitive radio network consisting of N SUs and a SBS in the presence of M EDs.

Finally, we evaluate the security-reliability tradeoff (SRT) of both the RrUS as well as of the CaUS and EaUS schemes, demonstrating that the CaUS scheme performs better than the EaUS scheme in terms of its SRT in the low-MER region, and the EaUS achieves the best SRT among the RrUS, CaUS and EaUS schemes in the high-MER region. To be specific, in the low-MER region the CaUS scheme achieves a lower OP than that of the EaUS scheme at a given IP constraint. Moreover, the CaUS scheme becomes more suitable for guarding against eavesdropping attacks in the face of more EDs upon increasing the number of the SUs of a given OP constraint in the low-MER region. By contrast, the EaUS scheme is more suitable for guaranteeing the security of wireless transmissions in the high-MER region.

The organization of this paper is as follows. In Section II, we briefly characterize the PLS of an EH aided cognitive radio (CR) network. In Section III, we carry out the SRT analyses of the RrUS, CaUS and EaUS schemes communicating over a Rayleigh channel. Our performance evaluations are detailed in Section IV. Finally, in Section V we conclude the paper.

II. User Scheduling For Energy-harvesting Cognitive Radio Networks

A. System Model

As shown in Fig. 1, we consider an underlay cognitive radio network consisting of a secondary network coexisting with a primary network, where the secondary network harvests energy from the primary network. The primary network supports a primary transmitter (PT) and primary receiver (PR) pair. In the secondary network, there are N SUs, denoted by SU_i, $i \in \{1, \cdots, N\}$, communicating with a secondary base station (SBS) in the presence of M eavesdroppers (EDs), denoted by E_k, $k \in \{1, \cdots, M\}$, where the EDs want to overhear the messages transmitted by the SUs. The EDs are equipped with multiple antennas. We assume that all the EDs have the same number of antennas, which is denoted by N_E. The SBS is also equipped with N_B receiving antennas, while each SU only has a single antenna. All links are modeled by Rayleigh fading [26], where the dashed lines and green lines in Fig. 1 represent the wiretap links (spanning from the SUs to the EDs) and energy harvesting links (spanning from the PT to the SUs), respectively. Let h_{pi}, h_{ir}, h_{iB_j} and $h_{iE_{k_l}}$, $i \in \{1, \cdots, N\}$, $k \in \{1, \cdots, M\}$, $j \in \{1, \cdots, N_B\}$, and $l \in \{1, \cdots, N_E\}$, respectively denote the channel gains of the $(PT\text{-}SU_i)$, $(SU_i\text{-}PR)$, $(SU_i\text{-}B_j)$ and $(SU_i\text{-}E_{k_l})$ links, which experience Rayleigh fading with respective variances of λ_{pi}, λ_{ir}, λ_{ij}, $\lambda_{iE_{k_l}}$, where $i \in \{1, \cdots, N\}$, $k \in \{1, \cdots, M\}$, $j \in \{1, \cdots, N_B\}$, and $l \in \{1, \cdots, N_E\}$, B_j and E_{k_l} represent the jth antenna of the SBS and lth antenna of E_k, respectively. Moreover, following [4], [22], [28], and [38], the interference received at the SBS from the PT can be considered to be a complex Gaussian random variable under the assumption that the primary signal may be generated by a random Gaussian codebook. Although the amplitude of the Gaussian codebook varies as a function of time, the secondary users can still harvest sufficient energy from the primary transmitter, provided that the energy harvesting time is much longer than the period of the Gaussian codebook. Moreover, the thermal noise at the SBS and E is also complex Gaussian distributed. Thus, the interference plus noise at the SBS and E can be modeled as a complex Gaussian random variable with zero mean and variance N_0. Moreover, for notational convenience, let U and E represent the set of N SUs and M EDs, respectively. Following [22], [38] and [39], we also assume that only a single SU is activated to perform its transmissions in order to reduce the multiple-access interference imposed on the PR.

We also assume that the $(SU_i\text{-}SBS)$ pair can complete its data transmission within two phases, denoted by αT and $(1-\alpha)T$, where α represents the portion occupied by the energy harvesting phase, T denotes the transmit slot duration, and $0 \leq \alpha \leq 1$. Specifically, all user nodes harvest energy from the radio frequency (RF) signals transmitted by PT in the first phase of duration αT. In the second phase $(1-\alpha)T$, the selected user node will transmit the data to its corresponding destination node. It is worth pointing out that if the SUs harvest energy from the SBS, the SBS has to transmit at sufficiently high power to guarantee the required level of energy harvested at the SUs, which may inflict harmful interference upon the primary receiver. Although power control can be used for reducing the interference, this will not only increase the system's complexity, but also limits the amount of energy harvested by the SUs. By contrast, in the sprit of [4] and [37], we assume that the SUs harvest as much energy as possible from the primary transmitter. Moreover, following [4], the energy harvested in the first phase of user node SU_i can be expressed as

$$E_i = \eta \alpha T P_T |h_{pi}|^2, \tag{1}$$

where η represents the energy conversion efficiency of the EH nodes, and $0 \leq \eta \leq 1$, P_T denotes the transmit power of the PT. It is pointed out that although the non-linear energy harvesting (EH) model conceived in [31] is more practical, it is analytically untractable [32]. Moreover, the non-linear model exhibits piecewise linearity, especially in the relatively low-power and high-power regimes, whilst the users relying entirely on EH may operate in the low-power regime, due to the limited efficiency of EH over wireless channels. Hence, the non-linear EH model of [31] can be roughly approximated by a linear energy harvesting model at relatively low powers, which has been widely adopted in the existing literature [4] and [33]-[36].

In this subsection, we assume that SU_i is selected to transmit its data to the SBS in the transmission slot. Thus, the instantaneous achievable rate of the $(SU_i\text{-}SBS)$ link can be expressed as

$$C_{U_iB} = (1-\alpha)\, T \log_2 \left(1 + \frac{P_i}{N_0} \sum_{j=1}^{N_D} \left| h_{iB_j} \right|^2 \right), \tag{2}$$

where P_i denotes the transmit power of SU_i, which depends both on the amount of energy harvested at the SU_i and on the interference temperature P_I experienced at the PR and expressed as

$$P_i = \min\left(\frac{\eta \alpha P_T |h_{pi}|^2}{1-\alpha}, \frac{P_I}{|h_{ir}|^2} \right). \tag{3}$$

Meanwhile, the signal transmitted by SU_i will be overheard by E, due to the broadcast nature of wireless channels. Similarly to (2), the instantaneous achievable rate of the $(SU_i\text{-}E_k)$ link can be written as

$$C_{U_iE_k} = (1-\alpha)\, T \log_2 \left(1 + \frac{P_i}{N_0} \sum_{l=1}^{N_E} \left| h_{iE_{k_l}} \right|^2 \right). \tag{4}$$

In this paper, we assume that the EDs intercept the transmission between the SUs and SBS cooperatively with the aid of maximal ratio combining (MRC). As a result, the instantaneous achievable rate of the wiretap channel can be expressed as

$$C_{U_iE} = (1-\alpha)\, T \log_2 \left(1 + \frac{P_i}{N_0} \sum_{k=1}^{M} \sum_{l=1}^{N_E} \left| h_{iE_{k_l}} \right|^2 \right). \tag{5}$$

B. User Scheduling Relying on Channel State Information

Scheduling criterion: This subsection details the channel-aware user scheduling (CaUS) scheme, where the user having the best link to the SBS will be chosen to transmit. Thus, the user scheduling criterion of the CaUS scheme can be expressed as:

$$u = \arg\max_i \sum_{j=1}^{N_B} \left| h_{iB_j} \right|^2, \tag{6}$$

where u represents the index of the selected user. Explicitly this scheduling only relies on the instantaneous CSI, without on the transmit power of the chosen user.

C. Joint Energy Harvesting and Channel State Information Based User Scheduling

Scheduling criterion: in this section, we present the energy-aware user scheduling (EaUS) scheme, wherein a user having the maximal instantaneous achievable rate C_{U_iB} will be selected to transmit its signal in the given time slot, which is formulated as

$$o = \arg\max_i C_{U_iB} = \arg\max_i \left(P_i \sum_{j=1}^{N_B} \left|h_{iB_j}\right|^2 \right), \qquad (7a)$$

where o denotes the index of the selected user.

Constraints: the transmit power P_i is constrained by:

$$\text{s.t.} \quad P_i = \min(\frac{\eta\alpha P_T |h_{pi}|^2}{1-\alpha}, \frac{P_I}{|h_{ir}|^2}). \qquad (7b)$$

Substituting (7b) into (7a) yields:

$$o = \arg\max_i \left[\min\left(\frac{\eta\alpha P_T |h_{pi}|^2}{1-\alpha} \sum_{j=1}^{N_B} \left|h_{iB_j}\right|^2, \frac{P_I}{|h_{ir}|^2} \sum_{j=1}^{N_B} \left|h_{iB_j}\right|^2 \right) \right]. \qquad (8)$$

Observe from (8) that the user scheduling criterion relies not only on the CSIs of the link spanning from the SU_i to the SBS, but also on the amount of energy harvested and on the maximum tolerable interference imposed on the PR.

III. Performance analysis over Rayleigh Fading Channels

In this section, we present our SRT analysis both for the CaUS as well as for the EaUS schemes for transmission over Rayleigh channels. For comparison, we also provide the SRT analysis of the traditional RrUS scheme. Based on [26], the SRT is quantified in terms of the IP and OP, respectively.

A. Conventional Round-robin User Scheduling

As a benchmarking scheme, this subsection provides the IP and OP analyses of the traditional RrUS scheme. In the spirit of [25]-[27], the OP of the RrUS scheme can be defined as

$$P_{\text{out}}^{\text{RrUS}} = \Pr\left(C_{U_bB} < R_o\right), \qquad (9)$$

where b denotes the index of the chosen user, and R_o represents the overall data rate of (SU_b-SBS) transmission. More specifically, following the literature [26], [27], a secrecy encoder encodes the source messages for transmission at a secrecy rate of R_s, which will generate extra redundancy for improving the PLS of wireless transmissions.

In the conventional RrUS scheme, each SU in the set will be chosen to transmit with an equal probability. Therefore, using the law of total probability [28], we can obtain the OP for the RrUS scheme as

$$P_{\text{out}}^{\text{RrUS}} = \sum_{i=1}^{N} \Pr\left(C_{U_iB} < R_o, b = i\right). \qquad (10)$$

As mentioned above, in the RrUS scheme, each SU has the same probability to be activated as the transmission node, and substituting (2) and (3) into (10) yields:

$$\begin{aligned} P_{\text{out}}^{\text{RrUS}} &= \sum_{i=1}^{N} \frac{1}{N} \Pr\left(P_i \sum_{j=1}^{N_B} \left|h_{iB_j}\right|^2 < \Delta_1 \right) \\ &= \sum_{i=1}^{N} \frac{1}{N} \Pr\left(\sum_{j=1}^{N_B} \left|h_{iB_j}\right|^2 < \frac{\Delta_1\Delta_2}{|h_{pi}|^2}, |h_{pi}|^2 \le \frac{P_I\Delta_2}{|h_{ir}|^2} \right) \\ &+ \sum_{i=1}^{N} \frac{1}{N} \Pr\left(\sum_{j=1}^{N_B} \left|h_{iB_j}\right|^2 < \frac{\Delta_1 |h_{ir}|^2}{P_I}, |h_{pi}|^2 > \frac{P_I\Delta_2}{|h_{ir}|^2} \right), \end{aligned} \qquad (11)$$

where $\Delta_1 = (2^{\frac{R_o}{(1-\alpha)T}} - 1)N_0$, and $\Delta_2 = \frac{1-\alpha}{\eta\alpha P_T}$. Then (11) can be reformulated as

$$P_{\text{out}}^{\text{RrUS}} = \sum_{i=1}^{N} \frac{1}{N} \left(I_0 + I_1\right), \qquad (12)$$

where I_0 and I_1 are given by

$$I_0 = \Pr\left(\sum_{j=1}^{N_B} \left|h_{iB_j}\right|^2 < \frac{\Delta_1\Delta_2}{|h_{pi}|^2}, |h_{pi}|^2 \le \frac{P_I\Delta_2}{|h_{ir}|^2} \right) \qquad (13)$$

and

$$I_1 = \Pr\left(\sum_{j=1}^{N_B} \left|h_{iB_j}\right|^2 < \frac{\Delta_1 |h_{ir}|^2}{P_I}, |h_{pi}|^2 > \frac{P_I\Delta_2}{|h_{ir}|^2} \right), \qquad (14)$$

respectively.

According to Appendix A, I_0 can be obtained as (15) at the top of the following page. Moreover, I_1 can be formulated as

$$\begin{aligned} I_1 =& \frac{2}{\lambda_{ir}} \sqrt{\frac{P_I\Delta_2\lambda_{ir}}{\lambda_{pi}}} K_1\left(2\sqrt{\frac{P_I\Delta_2}{\lambda_{ir}\lambda_{pi}}} \right) \\ &- \sum_{n=0}^{N_B-1} \frac{2}{n!} \frac{(\Delta_1/\lambda_{ij})^n}{P_I^n \lambda_{ir}} \left(\psi_0\psi_1^{-1}\right)^{\frac{1+n}{2}} K_{1+n}\left(2\sqrt{\psi_0\psi_1}\right). \end{aligned} \qquad (16)$$

Substituting (15) and (16) into (12), $P_{\text{out}}^{\text{RrUS}}$ can be obtained.

Based on [26], an intercept event occurs when the instantaneous achievable rate of the eavesdropper's channel becomes higher than $R_0 - R_s$. Therefore, the definition of the RrUS scheme's IP can be formulated as

$$P_{\text{int}}^{\text{RrUS}} = \Pr\left(C_{U_bE} > R_e\right), \qquad (17)$$

where R_e denotes the difference between R_o as well as R_s, and we have $R_e = R_o - R_s$.

Using the law of total probability [28], the IP of the RrUS scheme can be rewritten as

$$P_{\text{int}}^{\text{RrUS}} = \sum_{i=1}^{N} \Pr\left(C_{U_iE} > R_e, b = i\right). \qquad (18)$$

Similarly to (12), by combining (3) and (5), we arrive at

$$P_{\text{int}}^{\text{RrUS}} = \sum_{i=1}^{N} \frac{1}{N} \left(I_2 + I_3\right), \qquad (19)$$

$$I_0 = 1 - \frac{2}{\lambda_{pi}}\sqrt{\frac{P_I\Delta_2\lambda_{pi}}{\lambda_{ir}}}K_1\left(2\sqrt{\frac{P_I\Delta_2}{\lambda_{ir}\lambda_{pi}}}\right) - \sum_{n=0}^{N_B-1}\frac{2}{n!}\frac{(\Delta_1\Delta_2/\lambda_{ij})^n}{\lambda_{pi}}\left(\frac{\Delta_1\Delta_2\lambda_{pi}}{\lambda_{ij}}\right)^{\frac{1-n}{2}}K_{1-n}\left(2\sqrt{\frac{\Delta_1\Delta_2}{\lambda_{pi}\lambda_{ij}}}\right)$$
$$+\sum_{n=0}^{N_B-1}\frac{2}{n!}\frac{(\Delta_1\Delta_2/\lambda_{ij})^n}{\lambda_{pi}}\left(\frac{\Delta_1\Delta_2\lambda_{pi}}{\lambda_{ij}}+\frac{P_I\Delta_2\lambda_{pi}}{\lambda_{ir}}\right)^{\frac{1-n}{2}}K_{1-n}\left(2\sqrt{\frac{\Delta_1\Delta_2}{\lambda_{ij}\lambda_{pi}}+\frac{P_I\Delta_2}{\lambda_{ir}\lambda_{pi}}}\right) \quad (15)$$

$$I_2 = \sum_{n=0}^{MN_E-1}\frac{2}{n!\lambda_{pi}}\left(\frac{\Delta_3\Delta_2}{\lambda_{iE_k}}\right)^n\left(\frac{\lambda_{pi}\Delta_3\Delta_2}{\lambda_{iE_k}}\right)^{\frac{1-n}{2}}K_{1-n}\left(2\sqrt{\frac{\Delta_3\Delta_2}{\lambda_{iE_k}\lambda_{pi}}}\right)$$
$$-\sum_{n=0}^{MN_E-1}\frac{2}{n!\lambda_{pi}}\left(\frac{\Delta_3\Delta_2}{\lambda_{iE_k}}\right)^n\left(\frac{\lambda_{pi}\Delta_3\Delta_2}{\lambda_{iE_k}}+\frac{P_I\Delta_2\lambda_{pi}}{\lambda_{ir}}\right)^{\frac{1-n}{2}}K_{1-n}\left(2\sqrt{\frac{P_I\Delta_2}{\lambda_{ir}\lambda_{pi}}+\frac{\Delta_3\Delta_2}{\lambda_{iE_k}\lambda_{pi}}}\right) \quad (22)$$

where I_2 and I_3 can be formulated as

$$I_2 = \Pr\left(\sum_{k=1}^{M}\sum_{l=1}^{N_E}\left|h_{iE_{k_l}}\right|^2 > \frac{\Delta_3\Delta_2}{|h_{pi}|^2}, |h_{pi}|^2 \le \frac{P_I\Delta_2}{|h_{ir}|^2}\right) \quad (20)$$

and

$$I_3 = \Pr\left(\sum_{k=1}^{M}\sum_{l=1}^{N_E}\left|h_{iE_{k_l}}\right|^2 > \frac{\Delta_3|h_{ir}|^2}{P_I}, |h_{pi}|^2 > \frac{P_I\Delta_2}{|h_{ir}|^2}\right), \quad (21)$$

respectively, where $\Delta_3 = (2^{\frac{R_e}{(1-\alpha)T}} - 1)N_0$.

Based on Appendix B, I_2 can be expressed as (22) at the top of the following page, and I_3 can be given by

$$I_3 = \sum_{n=0}^{MN_E-1}\frac{2}{n!\lambda_{ir}}\left(\frac{\Delta_3}{P_I\lambda_{iE_k}}\right)^n\left(\psi_0\psi_2^{-1}\right)^{\frac{1+n}{2}}K_{1+n}\left(2\sqrt{\psi_0\psi_2}\right). \quad (23)$$

Therefore, substituting (22) and (23) into (19), $P_{\text{int}}^{\text{RrUS}}$ can be obtained.

B. Channel-aware User Scheduling

This subsection presents the SRT analysis of the channel-aware user scheduling (CaUS) scheme. In the CaUS scheme, similarly to (9), the OP of the CaUS scheme can be expressed as

$$P_{\text{out}}^{\text{CaUS}} = \Pr\left(C_{U_uB} < R_o\right). \quad (24)$$

Using the law of total probability [28], and substituting both (2) and (6) into (24), yields

$$P_{\text{out}}^{\text{CaUS}} = \sum_{i=1}^{N}\Pr\left(P_i\sum_{j=1}^{N_B}\left|h_{iB_j}\right|^2 < \Delta_1, \max_{g\in D, g\neq i}\sum_{j=1}^{N_B}\left|h_{gB_j}\right|^2 < \sum_{j=1}^{N_B}\left|h_{iB_j}\right|^2\right). \quad (25)$$

Combining (3) and (25), we arrive at

$$P_{\text{out}}^{\text{CaUS}} = \sum_{i=1}^{N}(T_0 + T_1), \quad (26)$$

where T_0 and T_1 can be expressed as

$$T_0 = \Pr\left(\sum_{j=1}^{N_B}\left|h_{iB_j}\right|^2 < \frac{\Delta_1\Delta_2}{|h_{pi}|^2}, |h_{pi}|^2 \le \frac{P_I\Delta_2}{|h_{ir}|^2}, \max_{g\in D, g\neq i}\sum_{j=1}^{N_B}\left|h_{gB_j}\right|^2 < \sum_{j=1}^{N_B}\left|h_{iB_j}\right|^2\right) \quad (27)$$

and

$$T_1 = \Pr\left(\sum_{j=1}^{N_B}\left|h_{iB_j}\right|^2 < \frac{\Delta_1|h_{ir}|^2}{P_I}, |h_{pi}|^2 > \frac{P_I\Delta_2}{|h_{ir}|^2}, \max_{g\in D, g\neq i}\sum_{j=1}^{N_B}\left|h_{gB_j}\right|^2 < \sum_{j=1}^{N_B}\left|h_{iB_j}\right|^2\right), \quad (28)$$

respectively.

Based on Appendix C, T_1 and T_0 can be formulated as (29) and (30) at the top of the following page, respectively.

Then, using (29) and (30), $P_{\text{out}}^{\text{CaUS}}$ can be obtained. Similarly to (17), we can express the IP of the CaUS scheme as

$$P_{\text{int}}^{\text{CaUS}} = \Pr\left(C_{U_uE} > R_e\right). \quad (31)$$

Combining (5) and (6), and relying on the law of total probability [28], (31) can be rewritten as

$$P_{\text{int}}^{\text{CaUS}} = \sum_{i=1}^{N}\Pr\left(P_i\sum_{k=1}^{M}\sum_{l=1}^{N_E}\left|h_{iE_{k_l}}\right|^2 > \Delta_3, \max_{g\in D, g\neq i}\sum_{j=1}^{N_B}\left|h_{gB_j}\right|^2 < \sum_{j=1}^{N_B}\left|h_{iB_j}\right|^2\right). \quad (32)$$

Similarly to (26), substituting (3) into (32), we arrive at

$$P_{\text{int}}^{\text{CaUS}} = \sum_{i=1}^{N}(T_2 + T_3), \quad (33)$$

$$T_1 = \sum_{S'} \frac{2\beta_1}{\lambda_{ir}\lambda_{ij}^{N_B}\left(N_B-1\right)!} \frac{(\beta_2+N_B-1)!}{(1/\lambda_{ij}+\beta_3)^{\beta_2+N_B}} \sqrt{\frac{P_I\Delta_2\lambda_{ir}}{\lambda_{pi}}} K_1\left(2\sqrt{\frac{P_I\Delta_2}{\lambda_{ir}\lambda_{pi}}}\right) - \sum_{S'}\sum_{k=0}^{\beta_2+N_B-1} \frac{2\beta_1}{\lambda_{ir}\lambda_{ij}^{N_B}(N_B-1)!}$$
$$\cdot \frac{(\beta_2+N_B-1)!(\Delta_1/P_I)^k}{k!(1/\lambda_{ij}+\beta_3)^{\beta_2+N_B-k}} \left(\frac{P_I\Delta_2}{\lambda_{pi}}\left(\frac{1}{\lambda_{ir}}+\frac{\Delta_1}{P_I}\left(\frac{1}{\lambda_{ij}}+\beta_3\right)\right)^{-1}\right)^{\frac{1+k}{2}} K_{1+k}\left(2\sqrt{\frac{P_I\Delta_2}{\lambda_{pi}}\left(\frac{1}{\lambda_{ir}}+\frac{\Delta_1}{P_I}\left(\frac{1}{\lambda_{ij}}+\beta_3\right)\right)}\right) \quad (29)$$

$$T_0 = \sum_{S'} \frac{\beta_1}{\lambda_{ij}^{N_B}\left(N_B-1\right)!} \frac{(\beta_2+N_B-1)!}{(1/\lambda_{ij}+\beta_3)^{\beta_2+N_B}} - \sum_{S'} \frac{2\beta_1}{\lambda_{pi}\lambda_{ij}^{N_B}\left(N_B-1\right)!} \frac{(\beta_2+N_B-1)!}{(1/\lambda_{ij}+\beta_3)^{\beta_2+N_B}} \sqrt{\frac{P_I\Delta_2\lambda_{pi}}{\lambda_{ir}}} K_1\left(2\sqrt{\frac{\psi_0}{\lambda_{ir}}}\right)$$
$$- \sum_{S'}\sum_{k=0}^{\beta_2+N_B-1} \frac{2\beta_1(\Delta_1\Delta_2)^k}{\lambda_{pi}\lambda_{ij}^{N_B}\left(N_B-1\right)!} \frac{(\beta_2+N_B-1)!}{k!(1/\lambda_{ij}+\beta_3)^{\beta_2+N_B-k}} (\psi_4\lambda_{pi})^{\frac{1-k}{2}} K_{1-k}\left(2\sqrt{\frac{\psi_4}{\lambda_{pi}}}\right)$$
$$+ \sum_{S'}\sum_{k=0}^{\beta_2+N_B-1} \frac{2\beta_1(\Delta_1\Delta_2)^{kk}}{\lambda_{pi}\lambda_{ij}^{N_B}(N_B-1)!} \frac{(\beta_2+N_B-1)!}{k!(1/\lambda_{ij}+\beta_3)^{\beta_2+N_B-k}} \left(\psi_4\lambda_{pi}+\frac{P_I\Delta_2\lambda_{pi}}{\lambda_{ir}}\right)^{\frac{1-k}{2}} K_{1-k}\left(2\sqrt{\frac{\psi_0}{\lambda_{ir}}+\frac{\psi_4}{\lambda_{pi}}}\right) \quad (30)$$

where T_2 and T_3 can be expressed as:

$$T_2 = \Pr\left(\sum_{k=1}^{M}\sum_{l=1}^{N_E}\left|h_{iE_{k_l}}\right|^2 > \frac{\Delta_3\Delta_2}{|h_{pi}|^2}, |h_{pi}|^2 \le \frac{P_I\Delta_2}{|h_{ir}|^2},\right.$$
$$\left.\max_{g\in D, g\neq i}\sum_{j=1}^{N_B}\left|h_{gB_j}\right|^2 < \sum_{j=1}^{N_B}\left|h_{iB_j}\right|^2\right) \quad (34)$$

and

$$T_3 = \Pr\left(\sum_{k=1}^{M}\sum_{l=1}^{N_E}\left|h_{iE_{k_l}}\right|^2 > \frac{\Delta_3|h_{ir}|^2}{P_I}, |h_{pi}|^2 > \frac{P_I\Delta_2}{|h_{ir}|^2},\right.$$
$$\left.\max_{g\in D, g\neq i}\sum_{j=1}^{N_B}\left|h_{gB_j}\right|^2 < \sum_{j=1}^{N_B}\left|h_{iB_j}\right|^2\right), \quad (35)$$

respectively.

Based on Appendix E, T_2 and T_3 can be formulated as

$$T_2 = \sum_{S'} \frac{\beta_1\left(\beta_2+N_B-1\right)!}{\lambda_{ij}^{N_B}\left(N_B-1\right)!}\left(\frac{1}{\lambda_{ij}}+\beta_3\right)^{-\beta_2-N_B} I_2 \quad (36)$$

and

$$T_3 = \sum_{S'} \frac{\beta_1\left(\beta_2+N_B-1\right)!}{\lambda_{ij}^{N_B}\left(N_B-1\right)!}\left(\frac{1}{\lambda_{ij}}+\beta_3\right)^{-\beta_2-N_B} I_3, \quad (37)$$

respectively.

Substituting (36) and (37) into (33), $P_{\text{int}}^{\text{CaUS}}$ can be obtained.

C. Energy-aware User Scheduling

In this subsection, we analyze the SRT of the proposed energy-aware user scheduling (EaUS) scheme. According to the definition in (9), the OP of the EaUS scheme can be formulated as:

$$P_{\text{out}}^{\text{EaUS}} = \Pr\left(C_{U_oB} < R_o\right). \quad (38)$$

Substituting (2) and (7) into (38) yields

$$P_{\text{out}}^{\text{EaUS}} = \Pr\left(\max_i\left(P_i\sum_{j=1}^{N_B}\left|h_{iB_j}\right|^2\right) < \Delta_1\right)$$
$$= \prod_i \Pr\left(P_i\sum_{j=1}^{N_B}\left|h_{iB_j}\right|^2 < \Delta_1\right). \quad (39)$$

Substituting (3) into (39), we arrive at

$$P_{\text{out}}^{\text{EaUS}} = \prod_i I_0 + \prod_i I_1. \quad (40)$$

Substituting (15) and (16) into (40), finally we obtain $P_{\text{out}}^{\text{EaUS}}$.

Upon relying on the definition of the IP defined in (17), the IP of the proposed EaUS scheme can be expressed as

$$P_{\text{int}}^{\text{EaUS}} = \Pr\left(C_{U_oE} > R_e\right). \quad (41)$$

Using (5), (7) and the law of total probability [28], (41) can be expressed as

$$P_{\text{int}}^{\text{EaUS}} = \sum_{i=1}^{N}\Pr\left(P_i\sum_{k=1}^{M}\sum_{l=1}^{N_E}\left|h_{iE_{k_l}}\right|^2 > \Delta_3,\right.$$
$$\left.\max_{t\in D, t\neq i} P_t\sum_{j=1}^{N_B}\left|h_{tj}\right|^2 < P_i\sum_{j=1}^{N_B}\left|h_{iB_j}\right|^2\right). \quad (42)$$

Upon substituting (3) into (42), we arrive at (43) at the top of the following page. However, it is challenging to obtain the closed-form expression of $Q_{1\_0}(x)$, $Q_{1\_1}(x)$, $Q_{3\_0}(y)$ and $Q_{3\_1}(y)$ of Appendix D. For simplicity, in the spirit of [24] and [29], it is shown that performing the optimal user selection for the SBS can be viewed as being equivalent to the random user selection for the EDs. We assume that $\sum_{l=1}^{N_E}\left|h_{oE_{k_l}}\right|^2$ can be represented by $\sum_{l=1}^{N_E}\left|h_{iE_{k_l}}\right|^2$. As a result, (41) can be rewritten

$$P_{\text{int}}^{\text{EaUS}}=\sum_{i=1}^{N}\underbrace{\Pr\left(\sum_{k=1}^{M}\sum_{l=1}^{N_E}\left|h_{iE_{k_l}}\right|^2>\frac{\Delta_3\Delta_2}{\left|h_{pi}\right|^2},\max_{t\in D,t\neq i}P_t\sum_{j=1}^{N_B}|h_{tj}|^2<\frac{|h_{pi}|^2}{\Delta_2}\sum_{j=1}^{N_B}\left|h_{iB_j}\right|^2,\left|h_{pi}\right|^2\leq\frac{P_I\Delta_2}{\left|h_{ir}\right|^2}\right)}_{W_0}$$
$$+\sum_{i=1}^{N}\underbrace{\Pr\left(\sum_{k=1}^{M}\sum_{l=1}^{N_E}\left|h_{iE_{k_l}}\right|^2>\frac{\Delta_3\left|h_{ir}\right|^2}{P_I},\max_{t\in D,t\neq i}P_t\sum_{j=1}^{N_B}|h_{tj}|^2<\frac{P_I}{\left|h_{ir}\right|^2}\sum_{j=1}^{N_B}\left|h_{iB_j}\right|^2,\left|h_{pi}\right|^2>\frac{P_I\Delta_2}{\left|h_{ir}\right|^2}\right)}_{W_1} \tag{43}$$

as

$$P_{\text{int}_1}^{\text{EaUS}}=\Pr\left(\sum_{k=1}^{M}\sum_{l=1}^{N_E}\left|h_{iE_{k_l}}\right|^2>\frac{\Delta_3\Delta_2}{\left|h_{po}\right|^2},\left|h_{po}\right|^2\leq\frac{P_I\Delta_2}{\left|h_{or}\right|^2}\right)+\Pr\left(\sum_{k=1}^{M}\sum_{l=1}^{N_E}\left|h_{iE_{k_l}}\right|^2>\frac{\Delta_3\left|h_{or}\right|^2}{P_I},\left|h_{po}\right|^2>\frac{P_I\Delta_2}{\left|h_{or}\right|^2}\right). \tag{44}$$

After further manipulations, (44) can be given by

$$P_{\text{int}_1}^{\text{EaUS}}=\sum_{n=0}^{MN_E-1}\frac{2}{n!\lambda_{or}}\left(\frac{\Delta_3}{P_I\lambda_{oE_k}}\right)^n\left(\psi_0\psi_2^{-1}\right)^{\frac{1+n}{2}}K_{1+n}\left(2\sqrt{\psi_0\psi_2}\right)+\sum_{n=0}^{MN_E-1}\frac{2}{n!\lambda_{po}}\left(\frac{\Delta_3\Delta_2}{\lambda_{oE_k}}\right)^n\left(\frac{\lambda_{po}\Delta_3\Delta_2}{\lambda_{oE_k}}\right)^{\frac{1-n}{2}}K_{1-n}\left(2\sqrt{\frac{\Delta_3\Delta_2}{\lambda_{oE_k}\lambda_{po}}}\right)+\sum_{n=0}^{MN_E-1}\frac{2}{n!\lambda_{po}}\left(\frac{\Delta_3\Delta_2}{\lambda_{oE_k}}\right)^n\left(\frac{\lambda_{po}\Delta_3\Delta_2}{\lambda_{oE_k}}+\frac{P_I\Delta_2\lambda_{po}}{\lambda_{or}}\right)^{\frac{1-n}{2}}K_{1-n}\left(2\sqrt{\frac{P_I\Delta_2}{\lambda_{or}\lambda_{po}}+\frac{\Delta_3\Delta_2}{\lambda_{oE_k}\lambda_{po}}}\right). \tag{45}$$

It is worth pointing out that it can be observed from (12), (26) and (40) that our SU scheduling schemes are designed for reducing the outage probability (OP) of wireless transmissions, and that the OP of the schemes conceived can be further reduced as the number of SUs increases. By contrast, increasing the number of SUs does not reduce the OP of the RRUS scheme. Moreover, observe from (19), (33) and (45) that the intercept probability (IP) of all schemes is equal, which means that the schemes advocated are unable to directly reduce the IP of wireless transmissions. However, according to our SRT analysis, the security of wireless transmissions can still be improved, since the reliability enhancement attained can be converted into a secrecy improvement. Moreover, the amount of energy harvested and used for the secondary transmission is beneficial both for the legitimate reception at the SBS as well as for the EDs. To be specific, in the high-MER region, the EaUS scheme outperforms the CaUS scheme in terms of its SRT, since the main channel gain is much higher than that of the wiretapping channel in the high-MER region. Hence, increasing the transmit power for the secondary transmission is more beneficial for the legitimate reception at the SBS. By contrast, in the low-MER region, the CaUS is capable of achieving a better SRT than that of the EaUS scheme. The CaUS scheme can still be used for protecting wireless transmissions by increasing the number of SUs even at very low MER. Generally speaking, the CaUS and EaUS schemes conceived are capable of flexible reconfiguration according to the different MER regions.

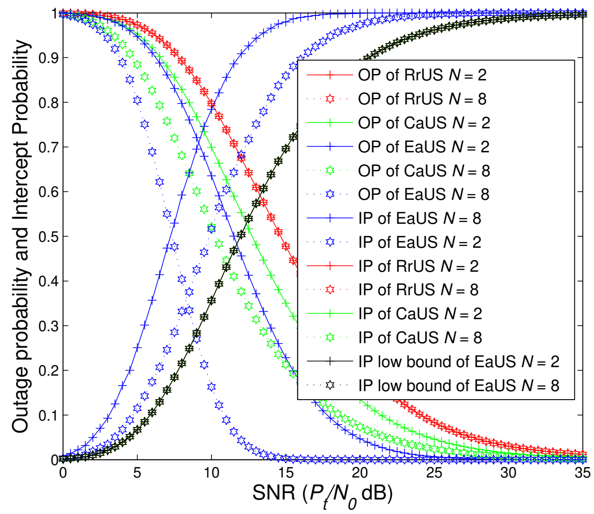

Fig. 2. IP and OP vs SNR (dB) of the conventional RrUS as well as the CaUS and EaUS schemes for different number of SUs N with λ_p = 0.2, λ_m = 1, λ_e = 0.2, M = 2, η = 0.4, α = 0.5, $N_B = N_E$ = 2, R_o = 1, R_s = 0.6.

IV. Performance Evaluation

In this section, we present our performance comparisons of the RrUS, CaUS and EaUS schemes in terms of their IP and OP. Specifically, the analytic OP of the RrUS, CaUS and EaUS schemes were evaluated by plotting (12), (26) and (40), respectively. Moreover, the IP of the RrUS, CaUS and EaUS schemes were obtained by using (19), (33) and (41), respectively. The lower bound IP of the EaUS scheme is provided by (46). The simulated IP and OP of the RrUS as well as of the CaUS and the EaUS schemes are provided for demonstrating the correctness of the theoretical results. In our numerical evaluations, we assume that $\lambda_{pi} = \alpha_{pi}\lambda_p$, $\lambda_{ir} = \alpha_{ir}\lambda_p$, $\lambda_{ij} = \alpha_{ij}\lambda_m$, $\lambda_{iE_{k_l}} = \alpha_{iE_{k_l}}\lambda_e$, $\alpha_{pi} = \alpha_{ir} = \alpha_{ij} = \alpha_{iE_{k_l}} = 1$, and P_I/N_0 = 10dB.

Fig. 2 shows the IP and OP vs SNR ($\frac{P_T}{N_0}$) of the conventional RrUS as well as of the CaUS and EaUS schemes for different number of SUs N. Observe from Fig. 2 that as the number of the SUs increases from N = 2 to 8, all the OP of the CaUS and of the EaUS schemes is significantly reduced, which shows that increasing the number of the SUs is beneficial for

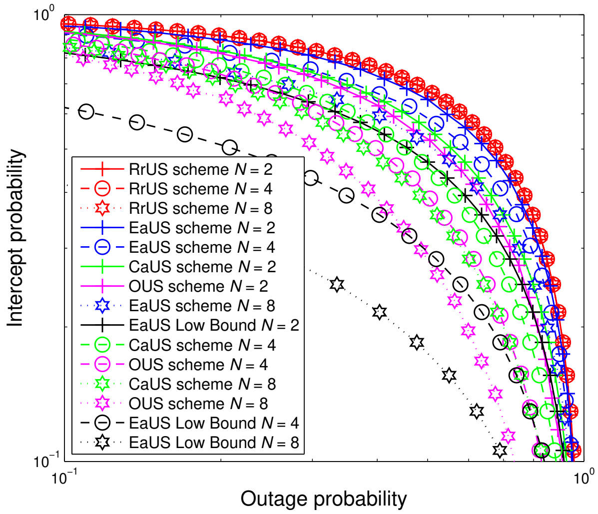

Fig. 3. IP vs OP of the conventional RrUS, OUS scheme [14] as well as the CaUS and EaUS schemes for different number of SUs N with λ_p = 0.2, λ_m = 1, λ_e = 0.2, M = 2, η = 0.4, α = 0.5, N_B = N_E = 2, R_o = 1, R_s = 0.6.

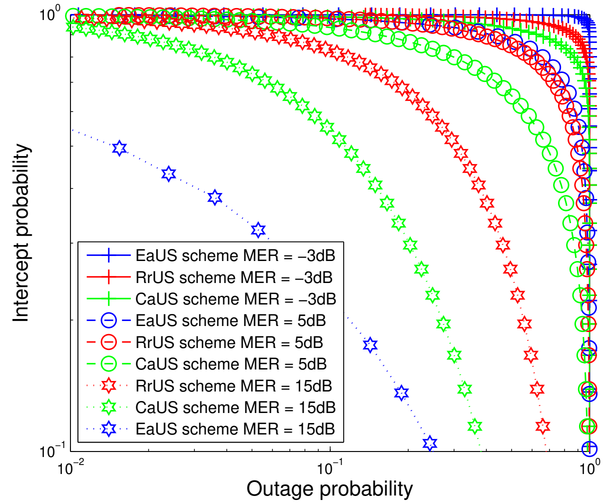

Fig. 5. IP vs OP of the conventional RrUS as well as the CaUS and EaUS schemes for different MER with λ_p = 0.2, N = 8, M = 2, η = 0.4, α = 0.5, N_B = N_E = 2, R_s = 0.6.

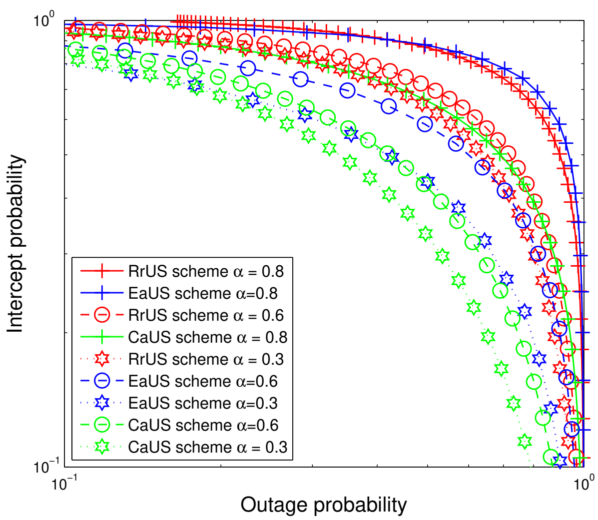

Fig. 4. IP vs OP of the conventional RrUS as well as the CaUS and EaUS schemes for different α with λ_p = 0.2, λ_m = 1, λ_e = 0.2, N = 8, M = 2, η = 0.4, N_B = N_E = 2, R_o = 1, R_s = 0.6.

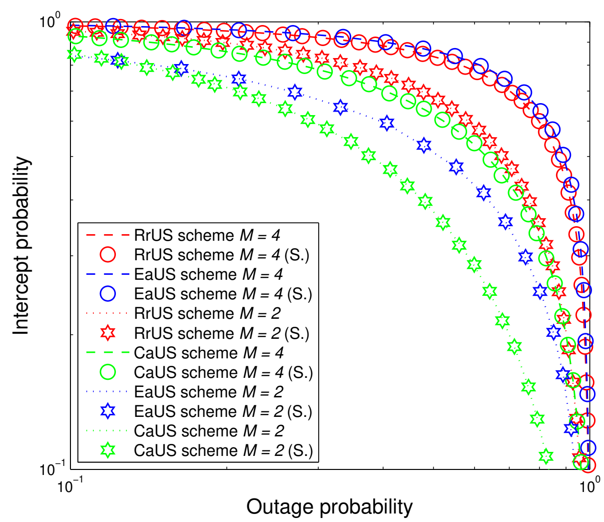

Fig. 6. IP vs OP of the conventional RrUS as well as the CaUS and EaUS schemes for different number of the EDs M with λ_p = 0.2, λ_m = 1, λ_e = 0.2, N = 8, η = 0.4, α = 0.5, N_B = N_E = 2, R_o = 1, R_s = 0.6.

the reliability of both the CaUS and of the EaUS schemes. Furthermore, Fig. 2 also shows that increasing the number of the SUs increases the IP of the EaUS scheme. Due to the fact that the user scheduling criterion of the EaUS scheme considers the product of the channel gains (spanning from the SUs to the SBS) and of the amount harvested energy, this indeed enhances the reliability of the SUs-SBS links, but simultaneously also increases the risk of the signals transmitted by a user being successfully intercepted. This is particularly likely to occur if the user has a low channel gain for the SU-SBS link, but a high harvested energy. Additionally, the EaUS scheme outperforms the CaUS and RrUS schemes in terms of its OP. However, the CaUS scheme achieves a lower IP than that of the EaUS scheme, showing a tradeoff between the security and reliability. Additionally, the black lines plotted in Fig. 2 can be used to assist us in verifying the analysis, where the amount of the harvested energy is not considered in the IP analysis of the EaUS scheme, which quantifies the lower bound of the IP of the EaUS. In order to take a more objective view of the CaUS and EaUS schemes, we analyze their SRT. In contrast to the CaUS and EaUS schemes, the users supported by the RrUS scheme take turns in communicating with the SBS. Hence, the IP and OP of the RrUS scheme remains unchanged, when the number of SUs increases from N = 2 to 8.

Fig. 3 depicts the IP vs OP of the conventional RrUS, of the full CSI based OUS [14] as well as of the CaUS and EaUS schemes for different number of SUs N. Observe in

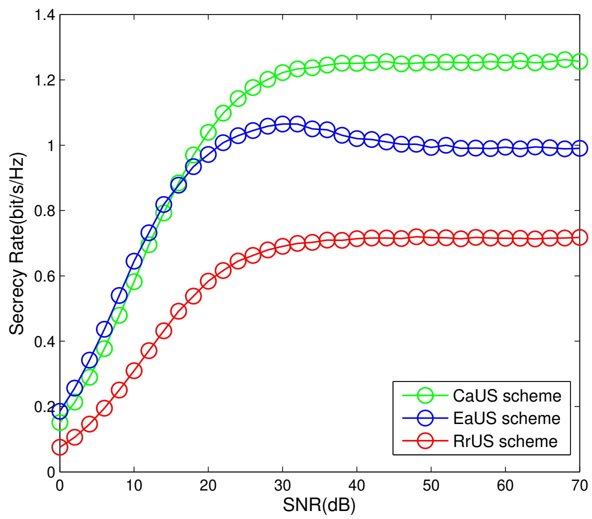

Fig. 7. Secrecy Rate vs SNR of the conventional RrUS as well as the CaUS and EaUS schemes with λ_p = 0.2, λ_m = 1, λ_e = 0.2, N = 8, η = 0.4, α = 0.5, N_B = N_E = 2, R_o = 1, R_s = 0.6.

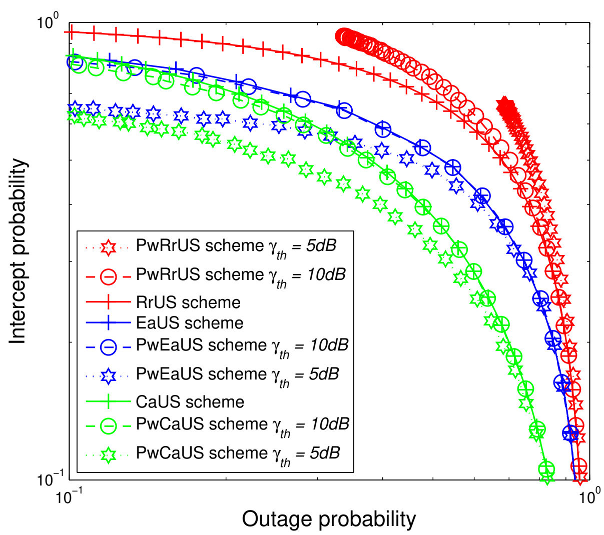

Fig. 8. IP vs OP of the conventional RrUS and piece-wise aided RrUS (PwRrUS) as well as the CaUS, piece-wise aided CaUS (PwCaUS), EaUS, and piece-wise aided EaUS (PwEaUS) schemes for different γ_{th} with λ_p = 0.2, λ_m = 1, λ_e = 0.2, N = 8, M = 2, η = 0.4, α = 0.5, N_B = N_E = 2, R_o = 1, R_s = 0.6.

Fig. 3 that as the number of SUs increases from N = 2 to 8, the SRT of the CaUS, of the EaUS and of OUS schemes is increased, showing that increasing the number of the SUs improves the SRT of the CaUS, EaUS and OUS schemes. We observe from Fig. 3 that the CaUS scheme outperforms the EaUS and RrUS scheme in terms of its SRT. This implies that the CaUS benefits more from the SUs-SBS cooperation in terms of enhancing the SRT of the networks investigated. However, the SRT of the RrUS scheme remains unchanged, when the number of SUs increases from N = 2 to 8. This is because the SU-SBS link of the RrUS scheme is selected randomly, without cooperation between the SUs. Additionally,

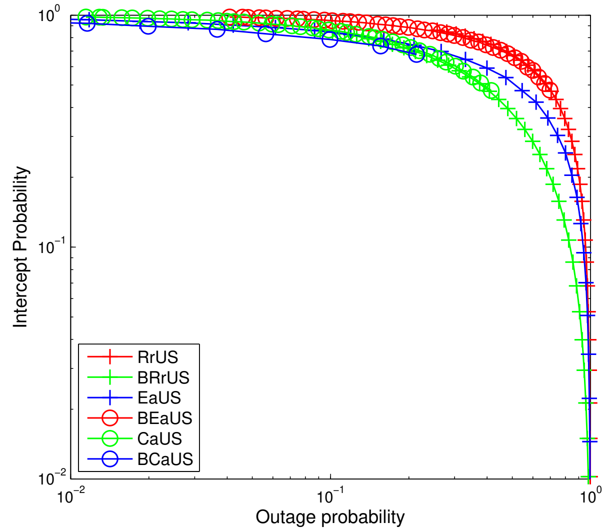

Fig. 9. IP and OP vs SNR (dB) of the conventional RrUS and battery aided RrUS (BRrUS) as well as the CaUS, battery aided CaUS (BCaUS), EaUS, and battery aided EaUS (BEaUS) schemes with λ_p = 0.2, λ_m = 1, λ_{ss} = 0.1, λ_e = 0.2, N = 8, M = 2, η = 0.4, α = 0.5, N_B = N_E = 2, R_o = 1, R_s = 0.6.

although the OUS scheme achieves the best SRT performance, this result is obtained at the cost of degrading the OP, whilst additionally relying not only on the instantaneous CSIs of the main links, but also on the instantaneous CSIs of the wiretap links. However, the CaUS and EaUS schemes do not require the instantaneous CSIs of the wiretap links, which are usually unavailable in practical systems.

In Fig. 4, we show the IP vs OP of the conventional RrUS as well as of the CaUS and EaUS schemes for different α values. Observe from Fig. 4 that the IP of the RrUS, the CaUS and of the EaUS schemes vary as α changes from α = 0.8 to 0.3. Thus, Fig. 4 demonstrates that varying the factor α improves the SRT of wireless transmissions in the EH-aided CR networks investigated. Additionally, Fig. 4 also demonstrates that the CaUS scheme attains the best SRT among the RrUS as well as the CaUS and EaUS schemes, as α varies from 0.8 to 0.3.

Fig. 5 illustrates the IP vs OP of the conventional RrUS as well as of the CaUS and EaUS schemes for different MER, where MER= λ_m/λ_e. Observe in Fig. 5 that increasing MER improves the SRT of the CaUS and EaUS schemes. In both MER = -3dB and MER = 5dB cases, the SRT of the CaUS scheme is best among the RrUS, CaUS and EaUS schemes. Furthermore, it can also be seen from Fig. 5 that the CaUS scheme can achieve a lower IP than the EaUS and RrUS schemes at a specific OP. In contrast to the EaUS scheme, this means that the SRT benefits from cooperation amongst the SUs by protecting against eavesdropping with the CaUS scheme in the low-MER region. By contrast, in MER = 15dB case, EaUS scheme outperforms the CaUS and RrUS schemes in terms its SRT, showing EaUS is more suitable for guarding wireless transmissions in the high-MER region.

In Fig. 6, we present the IP vs OP of the conventional RrUS as well as of the CaUS and EaUS schemes for different number of the EDs M. Observe from Fig. 6 that the SRT of the RrUS, the CaUS and EaUS schemes degrades as M varies from M = 2 to 8. Additionally, Fig. 6 also demonstrates that the CaUS scheme outperforms the RrUS and EaUS schemes in terms of its SRT. At a given OP constraint, although increasing the number of EDs naturally increases the risk of eavesdropping attacks, the CaUS scheme can be used to guard against the eavesdropping attacks by increasing the number of SUs, where OP constraint is a certain threshold of outage probability of wireless transmissions.

Fig. 7 shows the secrecy rate vs SNR of the conventional RrUS as well as of the CaUS and EaUS schemes. Observe from Fig. 7 that upon increasing the SNR, the secrecy rate of all schemes improves correspondingly, whereas the secrecy rate of all schemes remain at a steady state subsequently. Moreover, it can also be seen from Fig. 7 that the CaUS scheme outperforms the RrUS and EaUS schemes in terms of its secrecy rate, demonstrating its superiority.

Fig. 8 explores the IP vs OP of the conventional RrUS and PwRrUS as well as the CaUS, PwCaUS, EaUS, and PwEaUS schemes for different γ_{th}, where γ_{th} represents the ratio of the saturation threshold and N_0 of the piece-wise linear EH model [32]. It can be seen from Fig. 8 that upon varying the value of γ_{th}, the IP vs OP of the PwRrUS, PwCaUS, and PwEaUS schemes will be adjusted simultaneously. Moreover, observe from Fig. 8 that the IP vs OP relationships of the PwCaUS and PwEaUS schemes are approximately equivalent to that of the CaUS and EaUS schemes at γ_{th}=10dB. By contrast, the IP vs OP relationships of the PwRrUS scheme are similar to that of the RrUS scheme, when γ_{th} is above 8dB, because the SUs of the RrUS scheme are randomly selected.

In Fig. 9, we investigate the IP and OP vs SNR ($\frac{P_T}{N_0}$) of the conventional RrUS and BRrUS as well as the CaUS, BCaUS, EaUS, and BEaUS schemes. It is worth mentioning that in the battery aided schemes each SU can harvest energy not only from the PT, but also from the transmitting SU, and the remaining energy of the transmitting SU and other SUs will be stored in their own batteries [41], which can be represented by $P_i^s = \min(\max(\frac{\eta\alpha P_T|h_{pi}|^2}{1-\alpha} + P_i^s - \frac{P_I}{|h_{ir}|^2}, 0), P_B)$ and $P_j^s = \min(\frac{\eta\alpha P_T|h_{pj}|^2}{1-\alpha} + P_j^s + \eta P_i|h_{ij}|^2, P_B)$, respectively, where $P_i = \min(\frac{\eta\alpha P_T|h_{pi}|^2}{1-\alpha} + P_i^s, \frac{P_I}{|h_{ir}|^2})$, P_B is the maximum power stored in the battery, and P_B/N_0 is assumed to be 15dB, h_{ij} is the channel gain of the SU_i-SU_j link, $i, j \in \{1, \cdots, N\}$ and $i \neq j$. In this context we assumed that the links between the SUs are subjected to Rayleigh fading, all having the same variance of λ_{ss} = 0.1. Observe from Fig. 9 that the battery aided schemes have no obvious beneficial effect on enhancing the SRT, due to that the OP of the battery aided schemes may be considerably decreased, whereas the IP of these schemes will be increased accordingly.

V. Conclusions

In this paper, we investigated the PLS of a CR network consisting of a primary network and a secondary network in the presence of multiple EDs, where the nodes of the secondary network harvest energy from the transmitter of the primary network. We conceived the CaUS and EaUS schemes for improving the performance of the network investigated. To be specific, a user having the best link will be activated to transmit its signal to the SBS in the CaUS scheme. By contrast, a user having the maximal product of transmit power and channel gain will be selected as the transmitting user in the time-slot considered. The traditional RrUS scheme was used as our benchmarker. We derived the OP and IP expressions for the RrUS, CaUS and EaUS schemes. It was shown that the EaUS scheme outperforms the CaUS and RrUS schemes in terms of its OP. However, the CaUS scheme has the best SRT in the low-MER region. Additionally, the EaUS scheme has the worst IP of the three schemes. Finally, the security of wireless transmissions in the CaUS and EaUS schemes is upgraded upon increasing the number of SUs N.

Appendix A

Upon denoting $U = \sum_{j=1}^{N_B} |h_{iB_j}|^2$, $V = |h_{ir}|^2$ and $W = |h_{pi}|^2$, thus I_0=Pr($\sum_{j=1}^{N_B} |h_{iB_j}|^2 < \frac{\Delta_1\Delta_2}{|h_{pi}|^2}, |h_{pi}|^2 \leq \frac{P_I\Delta_2}{|h_{ir}|^2}$) and I_1 = Pr($\sum_{j=1}^{N_B} |h_{iB_j}|^2 < \frac{\Delta_1|h_{ir}|^2}{P_I}, |h_{pi}|^2 > \frac{P_I\Delta_2}{|h_{ir}|^2}$) can be formulated as

$$I_0 = \int_0^\infty F_U\left(\frac{\Delta_1\Delta_2}{w}\right) F_V\left(\frac{P_I\Delta_2}{w}\right) f_W(w)\, dw \quad \text{(A.1)}$$

and

$$I_1 = \int_0^\infty F_U\left(\frac{\Delta_1 v}{P_I}\right)\left(1 - F_W\left(\frac{P_I\Delta_2}{v}\right)\right) f_V(v)\, dv, \quad \text{(A.2)}$$

respectively, where $f_V(v)$ and $f_W(w)$ are the PDFs of the random variables (RVs) V and W, respectively. Moreover, $F_U(u)$, $F_V(v)$, and $F_W(w)$ are the cumulative distribution functions (CDFs) of RVs U, V, and W, respectively. Since the RVs V and W obey the exponential distribution, the PDFs of RVs V and W are $f_V(v) = \frac{1}{\lambda_{ir}}\exp(-\frac{v}{\lambda_{ir}})$ and $f_W(w) = \frac{1}{\lambda_{pi}}\exp(-\frac{w}{\lambda_{pi}})$, respectively. Moreover, the CDFs of RVs V and W are $F_V(v) = 1 - \exp(-\frac{v}{\lambda_{ir}})$ and $F_W(w) = 1 - \exp(-\frac{w}{\lambda_{pi}})$, respectively.

According to [30], the CDF of U can be formulated as

$$F_U(u) = 1 - \exp\left(-\frac{u}{\lambda_{ij}}\right)\sum_{n=0}^{N_B-1}\frac{1}{n!}\left(\frac{u}{\lambda_{ij}}\right)^n. \quad \text{(A.3)}$$

Thus, (A.3) and (A.4) can be rewritten as

$$I_0 = \int_0^\infty\left(1 - \exp\left(-\frac{\Delta_1\Delta_2}{\lambda_{ij}w}\right)\sum_{n=0}^{N_B-1}\frac{1}{n!}\left(\frac{\Delta_1\Delta_2}{\lambda_{ij}w}\right)^n\right) \times\left(1 - \exp\left(-\frac{P_I\Delta_2}{\lambda_{ir}w}\right)\right)\frac{1}{\lambda_{pi}}\exp\left(-\frac{w}{\lambda_{pi}}\right)dw \quad \text{(A.4)}$$

and

$$I_1 = \int_0^\infty\left(1 - \exp\left(-\frac{\Delta_1 v}{\lambda_{ij}P_I}\right)\sum_{n=0}^{N_B-1}\frac{1}{n!}\left(\frac{\Delta_1 v}{\lambda_{ij}P_I}\right)^n\right) \times\frac{1}{\lambda_{ir}}\exp\left(-\frac{P_I\Delta_2}{\lambda_{pi}v} - \frac{v}{\lambda_{ir}}\right)dv, \quad \text{(A.5)}$$

respectively.

Based on [40], I_0 and I_1 can be expressed as

$$I_0=1-\frac{2}{\lambda_{pi}}\sqrt{\frac{P_I\Delta_2\lambda_{pi}}{\lambda_{ir}}}K_1\left(2\sqrt{\frac{P_I\Delta_2}{\lambda_{ir}\lambda_{pi}}}\right)-\sum_{n=0}^{N_B-1}\frac{2}{n!}\frac{(\Delta_1\Delta_2/\lambda_{ij})^n}{\lambda_{pi}}\left(\frac{\Delta_1\Delta_2\lambda_{pi}}{\lambda_{ij}}\right)^{\frac{1-n}{2}}K_{1-n}\left(2\sqrt{\frac{\Delta_1\Delta_2}{\lambda_{pi}\lambda_{ij}}}\right)+\sum_{n=0}^{N_B-1}\frac{2}{n!}\frac{(\Delta_1\Delta_2/\lambda_{ij})^n}{\lambda_{pi}}\left(\frac{\Delta_1\Delta_2\lambda_{pi}}{\lambda_{ij}}+\frac{P_I\Delta_2\lambda_{pi}}{\lambda_{ir}}\right)^{\frac{1-n}{2}}K_{1-n}\left(2\sqrt{\frac{\Delta_1\Delta_2}{\lambda_{ij}\lambda_{pi}}+\frac{P_I\Delta_2}{\lambda_{ir}\lambda_{pi}}}\right) \tag{A.6}$$

and

$$I_1=\frac{2}{\lambda_{ir}}\sqrt{\frac{P_I\Delta_2\lambda_{ir}}{\lambda_{pi}}}K_1\left(2\sqrt{\frac{P_I\Delta_2}{\lambda_{ir}\lambda_{pi}}}\right)-\sum_{n=0}^{N_B-1}\frac{2}{n!}\frac{(\Delta_1/\lambda_{ij})^n}{P_I^n\lambda_{ir}}\left(\psi_0\psi_1^{-1}\right)^{\frac{1+n}{2}}K_{1+n}\left(2\sqrt{\psi_0\psi_1}\right), \tag{A.7}$$

respectively, where $K_v(z)$ is the modified Bessel function, $\psi_0=\frac{P_I\Delta_2}{\lambda_{pi}}$, and $\psi_1=\frac{1}{\lambda_{ir}}+\frac{\Delta_1}{P_I\lambda_{ij}}$.

Appendix B

Let U, V and W denote $\sum_{k=1}^{M}\sum_{l=1}^{N_E}|h_{iE_{k_l}}|^2$, $|h_{ir}|^2$, and $|h_{pi}|^2$, respectively. As mentioned above, the RVs V and W are exponentially distributed. For simplicity, we assume that $\sum_{k=1}^{M}\sum_{l=1}^{N_E}\left|h_{iE_{k_l}}\right|^2$ for different l value have the same variance λ_{iE_k}. Moreover, RVs U, V and W are independent of each other, for different i. Thus, we can rewrite $I_2=\Pr(\sum_{k=1}^{M}\sum_{l=1}^{N_E}|h_{iE_{k_l}}|^2>\frac{\Delta_3\Delta_2}{|h_{pi}|^2},|h_{pi}|^2\le\frac{P_I\Delta_2}{|h_{ir}|^2})$ and $I_3=\Pr(\sum_{k=1}^{M}\sum_{l=1}^{N_E}|h_{iE_{k_l}}|^2>\frac{\Delta_3|h_{ir}|^2}{P_I},|h_{pi}|^2>\frac{P_I\Delta_2}{|h_{ir}|^2})$ as

$$I_2=\int_0^\infty\left(1-F_U\left(\frac{\Delta_3\Delta_2}{w}\right)\right)F_V\left(\frac{P_I\Delta_2}{w}\right)f_W(w)\,dw \tag{B.1}$$

and

$$I_3=\int_0^\infty\left(1-F_U\left(\frac{\Delta_3 v}{P_I}\right)\right)\left(1-F_W\left(\frac{P_I\Delta_2}{v}\right)\right)f_V(v)\,dv, \tag{B.2}$$

respectively, where $F_U(u)$ can be given by

$$F_U(u)=1-\exp\left(-\frac{u}{\lambda_{iE_k}}\right)\sum_{n=0}^{MN_E-1}\frac{1}{n!}\left(\frac{u}{\lambda_{iE_k}}\right)^n. \tag{B.3}$$

Furthermore, (B.1) and (B.2) can be expanded as

$$I_2=\int_0^\infty\left(\exp\left(-\frac{\Delta_3\Delta_2}{\lambda_{iE_k}w}\right)\sum_{n=0}^{MN_E-1}\frac{1}{n!}\left(\frac{\Delta_3\Delta_2}{\lambda_{iE_k}w}\right)^n\right)\left(1-\exp\left(-\frac{P_I\Delta_2}{\lambda_{ir}w}\right)\right)\frac{1}{\lambda_{pi}}\exp\left(-\frac{w}{\lambda_{pi}}\right)dw \tag{B.4}$$

and

$$I_3=\int_0^\infty\exp\left(-\frac{\Delta_3 v}{\lambda_{iE_k}P_I}-\frac{P_I\Delta_2}{\lambda_{pi}v}-\frac{v}{\lambda_{ir}}\right)\left(\sum_{n=0}^{MN_E-1}\frac{1}{n!}\left(\frac{\Delta_3 v}{\lambda_{iE_k}P_I}\right)^n\right)\frac{1}{\lambda_{ir}}dv, \tag{B.5}$$

respectively.

Finally, I_2 and I_3 can be obtained as

$$I_2=\sum_{n=0}^{MN_E-1}\frac{2}{n!\lambda_{pi}}\left(\frac{\Delta_3\Delta_2}{\lambda_{iE_k}}\right)^n\left(\frac{\lambda_{pi}\Delta_3\Delta_2}{\lambda_{iE_k}}\right)^{\frac{1-n}{2}}K_{1-n}\left(2\sqrt{\frac{\Delta_3\Delta_2}{\lambda_{iE_k}\lambda_{pi}}}\right)-\sum_{n=0}^{MN_E-1}\frac{2}{n!\lambda_{pi}}\left(\frac{\Delta_3\Delta_2}{\lambda_{iE_k}}\right)^n\left(\frac{\lambda_{pi}\Delta_3\Delta_2}{\lambda_{iE_k}}+\frac{P_I\Delta_2\lambda_{pi}}{\lambda_{ir}}\right)^{\frac{1-n}{2}}K_{1-n}\left(2\sqrt{\frac{P_I\Delta_2}{\lambda_{ir}\lambda_{pi}}+\frac{\Delta_3\Delta_2}{\lambda_{iE_k}\lambda_{pi}}}\right) \tag{B.6}$$

and

$$I_3=\sum_{n=0}^{MN_E-1}\frac{2}{n!\lambda_{ir}}\left(\frac{\Delta_3}{P_I\lambda_{iE_k}}\right)^n\left(\psi_0\psi_2^{-1}\right)^{\frac{1+n}{2}}K_{1+n}\left(2\sqrt{\psi_0\psi_2}\right), \tag{B.7}$$

respectively, $\psi_2=\frac{1}{\lambda_{ir}}+\frac{\Delta_3}{\lambda_{iE_k}P_I}$.

Appendix C

Upon denoting $U=\sum_{j=1}^{N_B}|h_{iB_j}|^2$, $V=|h_{ir}|^2$, and $W=|h_{pi}|^2$, T_0 and T_1 can be formulated as

$$T_0=\int_0^\infty\int_0^{\frac{\Delta_1\Delta_2}{w}}\left(\prod_{g\in D,g\neq i}\Pr\left(\sum_{j=1}^{N_B}\left|h_{gB_j}\right|^2<u\right)\right)\Pr\left(|h_{ir}|^2\le\frac{P_I\Delta_2}{w}\right)f_U(u)\,f_W(w)\,dudw \tag{C.1}$$

and

$$T_1=\int_0^\infty\int_0^{\frac{\Delta_1 v}{P_I}}\left(\prod_{g\in D,g\neq i}\Pr\left(\sum_{j=1}^{N_B}\left|h_{gB_j}\right|^2<u\right)\right)\Pr\left(|h_{pi}|^2>\frac{P_I\Delta_2}{v}\right)f_U(u)\,f_V(v)\,dudv, \tag{C.2}$$

respectively.

Substituting (A.3) into (C.1), T_0 can be expanded as

$$\begin{aligned}T_0&=\int_0^\infty\int_0^{\frac{\Delta_1\Delta_2}{w}}\left(\prod_{g\in D,g\neq i}\Pr\left(\sum_{j=1}^{N_B}\left|h_{gB_j}\right|^2<u\right)\right)\Pr\left(|h_{ir}|^2\le\frac{P_I\Delta_2}{w}\right)f_U(u)\,f_W(w)\,dudw\\&=\sum_{S'}\int_0^\infty\int_0^{\frac{\Delta_1\Delta_2}{w}}\frac{\beta_1u^{\beta_2+N_B-1}}{\lambda_{pi}\lambda_{ij}^{N_B}(N_B-1)!}\exp\left(-\frac{w}{\lambda_{pi}}\right)\exp\left(-\left(\frac{1}{\lambda_{ij}}+\beta_3\right)u\right)dudw\\&\quad-\sum_{S'}\int_0^\infty\int_0^{\frac{\Delta_1\Delta_2}{w}}\frac{\beta_1u^{\beta_2+N_B-1}}{\lambda_{pi}\lambda_{ij}^{N_B}(N_B-1)!}\exp\left(-\left(\frac{1}{\lambda_{ij}}+\beta_3\right)u\right)\exp\left(-\frac{w}{\lambda_{pi}}-\frac{P_I\Delta_2}{w\lambda_{ir}}\right)dudw.\end{aligned} \tag{C.3}$$

After further manipulations, T_0 can be expressed as

$$T_0=\sum_{S'}\frac{\beta_1}{\lambda_{ij}^{N_B}(N_B-1)!}\frac{(\beta_2+N_B-1)!}{(1/\lambda_{ij}+\beta_3)^{\beta_2+N_B}}$$
$$-\sum_{S'}\frac{2\beta_1}{\lambda_{pi}\lambda_{ij}^{N_B}(N_B-1)!}\frac{(\beta_2+N_B-1)!}{(1/\lambda_{ij}+\beta_3)^{\beta_2+N_B}}\sqrt{\frac{P_I\Delta_2\lambda_{pi}}{\lambda_{ir}}}K_1\left(2\sqrt{\frac{\psi_0}{\lambda_{ir}}}\right)$$
$$-\sum_{S'}\sum_{k=0}^{\beta_2+N_B-1}\frac{2\beta_1(\Delta_1\Delta_2)^k}{\lambda_{pi}\lambda_{ij}^{N_B}(N_B-1)!}\frac{(\beta_2+N_B-1)!}{k!(1/\lambda_{ij}+\beta_3)^{\beta_2+N_B-k}}$$
$$(\psi_4\lambda_{pi})^{\frac{1-k}{2}}K_{1-k}\left(2\sqrt{\frac{\psi_4}{\lambda_{pi}}}\right)$$
$$+\sum_{S'}\sum_{k=0}^{\beta_2+N_B-1}\frac{2\beta_1(\Delta_1\Delta_2)^{kk}}{\lambda_{pi}\lambda_{ij}^{N_B}(N_B-1)!}\frac{(\beta_2+N_B-1)!}{k!(1/\lambda_{ij}+\beta_3)^{\beta_2+N_B-k}}$$
$$\left(\psi_4\lambda_{pi}+\frac{P_I\Delta_2\lambda_{pi}}{\lambda_{ir}}\right)^{\frac{1-k}{2}}K_{1-k}\left(2\sqrt{\frac{P_I\Delta_2}{\lambda_{pi}\lambda_{ir}}+\frac{\psi_4}{\lambda_{pi}}}\right), \quad (C.4)$$

where $\psi_4=(1/\lambda_{ij}+\beta_3)\,\Delta_1\Delta_2$. Similarly to (C.4), T_1 can be formulated as

$$T_1=\sum_{S'}\frac{2\beta_1}{\lambda_{ir}\lambda_{ij}^{N_B}(N_B-1)!}\frac{(\beta_2+N_B-1)!}{\left(\frac{1}{\lambda_{ij}}+\beta_3\right)^{\beta_2+N_B}}\sqrt{\frac{P_I\Delta_2\lambda_{ir}}{\lambda_{pi}}}K_1\left(2\sqrt{\frac{P_I\Delta_2}{\lambda_{ir}\lambda_{pi}}}\right)$$
$$-\sum_{S'}\sum_{k=0}^{\beta_2+N_B-1}\frac{2\beta_1}{\lambda_{ir}\lambda_{ij}^{N_B}\,(N_B-1)!}\left(\frac{P_I\Delta_2}{\lambda_{pi}}\left(\frac{1}{\lambda_{ir}}+\frac{\Delta_1}{P_I}\left(\frac{1}{\lambda_{ij}}+\beta_3\right)\right)^{-1}\right)^{\frac{1+k}{2}}$$
$$\frac{(\beta_2+N_B-1)!(\Delta_1/P_I)^k}{k!(1/\lambda_{ij}+\beta_3)^{\beta_2+N_B-k}}K_{1+k}\left(2\sqrt{\frac{P_I\Delta_2}{\lambda_{pi}}\left(\frac{1}{\lambda_{ir}}+\frac{\Delta_1}{P_I}\left(\frac{1}{\lambda_{ij}}+\beta_3\right)\right)}\right), \quad (C.5)$$

where $\beta_1 = \frac{(|D|-1)!}{\prod_{i=1}^{N_B+1} n_i!}\prod_{j=1}^{N_B}(-\frac{1}{\lambda_g{}^{j-1}(j-1)!})^{n_j}$, $\beta_2 = \sum_{j=1}^{N_B} n_j(j-1)$, $\beta_3 = \frac{1}{\lambda_g}(|D|-1+n_{N_B+1})$ and $S'=\{(n_1,n_2,\cdots,n_{N_B+1})|\sum_{i=1}^{N_B+1} n_i=|D|-1\}$.

APPENDIX D

Let W_0 and W_1 denote the first part and the second part of (43), respectively. For notational convenience, we introduce the shorthand of $x=|h_{pi}|^2$, $y=|h_{ir}|^2$, $z=|h_{pt}|^2$ and $v=|h_{tr}|^2$. Thus, W_0 and W_1 can be rewritten as

$$W_0=\int_0^\infty\frac{Q_0(x)Q_1(x)}{\lambda_{pi}}\left(\exp\left(-\frac{x}{\lambda_{pi}}\right)-\exp\left(-\frac{1}{\lambda_{ir}}\frac{P_I\Delta_2}{x}-\frac{x}{\lambda_{pi}}\right)\right)dx \quad (D.1)$$

and

$$W_1=\int_0^\infty\frac{Q_2(y)\,Q_3(y)}{\lambda_{ir}}\exp\left(-\frac{1}{\lambda_{pi}}\frac{P_I\Delta_2}{y}-\frac{y}{\lambda_{ir}}\right)dy, \quad (D.2)$$

respectively, where $Q_0(x)=\Pr(\sum_{k=1}^{M}\sum_{l=1}^{N_E}|h_{iE_{k_l}}|^2>\frac{\Delta_3\Delta_2}{x})$, $Q_1(x)=\prod_{t\in D,t\neq i}(Q_{1\_0}(x)+Q_{1\_1}(x))$, $Q_{1\_0}(x)=\int_0^\infty\frac{Q_{1\_0\_0}(x,z)}{\lambda_{pt}}(\exp(-\frac{z}{\lambda_{pt}})-\exp(-\frac{1}{\lambda_{tr}}\frac{P_I\Delta_2}{z}-\frac{z}{\lambda_{pt}}))dz$, $Q_{1\_1}(x)=\int_0^\infty\frac{Q_{1\_1\_0}(x,v)}{\lambda_{tr}}\exp(-\frac{1}{\lambda_{pt}}\frac{P_I\Delta_2}{v}-\frac{v}{\lambda_{tr}})dv$, $Q_{1\_0\_0}(x,z)=\Pr(\sum_{j=1}^{N_B}|h_{tj}|^2<\frac{x}{z}\sum_{j=1}^{N_B}|h_{iB_j}|^2)$, $Q_{1\_1\_0}(x,v)=\Pr(\sum_{j=1}^{N_B}|h_{tj}|^2<\frac{xv}{\Delta_2P_I}\sum_{j=1}^{N_B}|h_{iB_j}|^2)$, $Q_2(y)=\Pr(\sum_{k=1}^{M}\sum_{l=1}^{N_E}|h_{iE_{k_l}}|^2>\frac{\Delta_3 y}{P_I})$, $Q_3(y)=\prod_{t\in D,t\neq i}(Q_{3\_0}(y)+Q_{3\_1}(y))$, $Q_{3\_0}(y)=\int_0^\infty\frac{Q_{3\_0\_0}(y,z)}{\lambda_{pt}}(\exp(-\frac{z}{\lambda_{pt}})-\exp(-\frac{1}{\lambda_{tr}}\frac{P_I\Delta_2}{z}-\frac{z}{\lambda_{pt}}))dz$, $Q_{3\_1}(y)=\int_0^\infty\frac{Q_{3\_1\_0}(y,v)}{\lambda_{tr}}\exp(-\frac{1}{\lambda_{pt}}\frac{P_I\Delta_2}{v}-\frac{v}{\lambda_{tr}})dv$, $Q_{3\_0\_0}(y,z)=\Pr(\sum_{j=1}^{N_B}|h_{tj}|^2<\frac{\Delta_2P_I}{yz}\sum_{j=1}^{N_B}|h_{iB_j}|^2)$, and $Q_{3\_1\_0}(y,v)=\Pr(\sum_{j=1}^{N_B}|h_{tj}|^2<\frac{v}{y}\sum_{j=1}^{N_B}|h_{iB_j}|^2)$.

Based on (B.3), $Q_0(x)$ and $Q_2(y)$ can be obtained as

$$Q_0(x)=\exp\left(-\frac{\Delta_3\Delta_2}{\lambda_{iE_k}x}\right)\sum_{n=0}^{MN_E-1}\frac{1}{n!}\left(\frac{\Delta_3\Delta_2}{\lambda_{iE_k}x}\right)^n. \quad (D.3)$$

and

$$Q_2(y)=\exp\left(-\frac{\Delta_3 y}{P_I\lambda_{iE_k}}\right)\sum_{n=0}^{MN_E-1}\frac{1}{n!}\left(\frac{\Delta_3 y}{P_I\lambda_{iE_k}}\right)^n. \quad (D.4)$$

respectively.

Using (C.3), $Q_{1\_0\_0}(x,z)$, $Q_{1\_1\_0}(x,v)$, $Q_{3\_0\_0}(y,z)$ and $Q_{3\_1\_0}(y,v)$ can be obtained as

$$Q_{1\_0\_0}(x,z)=1-\sum_{n=0}^{N_B-1}a_0(n)\left(\frac{x}{z}\right)^n\left(\frac{1}{\lambda_{ij}}+\frac{1}{\lambda_{tj}}\frac{x}{z}\right)^{-N_B-n} \quad (D.5)$$

and

$$Q_{1\_1\_0}(x,v)=1-\sum_{n=0}^{N_B-1}a_1(n)\,(xv)^n\left(\frac{1}{\lambda_{ij}}+\frac{1}{\lambda_{tj}\Delta_2P_I}xv\right)^{-N_B-n} \quad (D.6)$$

and

$$Q_{3\_0\_0}(y,z)=1-\sum_{n=0}^{N_B-1}a_2(n)\left(\frac{1}{yz}\right)^n\left(\frac{1}{\lambda_{ij}}+\frac{\Delta_2P_I}{\lambda_{tj}}\frac{1}{yz}\right)^{-N_B-n} \quad (D.7)$$

and

$$Q_{3\_1\_0}(y,v)=1-\sum_{n=0}^{N_B-1}a_0(n)\left(\frac{v}{y}\right)^n\left(\frac{1}{\lambda_{ij}}+\frac{1}{\lambda_{tj}}\frac{v}{y}\right)^{-N_B-n}, \quad (D.8)$$

respectively, where $a_0(n)=\frac{(N_B+n-1)!}{n!(N_B-1)!}(\frac{1}{\lambda_{ij}})^{N_B}(\frac{1}{\lambda_{tj}})^n$, $a_1(n)=\frac{(N_B+n-1)!}{n!(N_B-1)!}(\frac{1}{\lambda_{ij}})^{N_B}(\frac{1}{\lambda_{tj}\Delta_2P_I})^n$, and $a_2(n)=\frac{(N_B+n-1)!}{n!(N_B-1)!}(\frac{1}{\lambda_{ij}})^{N_B}(\frac{\Delta_2P_I}{\lambda_{tj}})^n$.

APPENDIX E

Upon denoting $X=|h_{pi}|^2$, and $Y=|h_{ir}|^2$, since all RVs $|h_{iE_{k_l}}|^2$, $|h_{iB_j}|^2$, X, and Y are independent of each other, T_2

and T_3 can be rewritten as

$$T_2=\int_0^\infty \Pr\left(\sum_{k=1}^{M}\sum_{l=1}^{N_E}\left|h_{iE_{k_l}}\right|^2>\frac{\Delta_3\Delta_2}{x}\right)\Pr\left(\left|h_{ir}\right|^2\leq\frac{P_I\Delta_2}{x}\right)\underbrace{\Pr\left(\max_{g\in D,g\neq i}\sum_{j=1}^{N_B}\left|h_{gB_j}\right|^2<\sum_{j=1}^{N_B}\left|h_{iB_j}\right|^2\right)}_{T_{2\_0}}f_X(x)\,dx \quad \text{(E.1)}$$

and

$$T_3=\int_0^\infty \Pr\left(\sum_{k=1}^{M}\sum_{l=1}^{N_E}\left|h_{iE_{k_l}}\right|^2>\frac{\Delta_3 y}{P_I}\right)\Pr\left(\left|h_{pi}\right|^2>\frac{P_I\Delta_2}{y}\right)\underbrace{\Pr\left(\max_{g\in D,g\neq i}\sum_{j=1}^{N_B}\left|h_{gB_j}\right|^2<\sum_{j=1}^{N_B}\left|h_{iB_j}\right|^2\right)}_{T_{2\_0}}f_Y(y)\,dy, \quad \text{(E.2)}$$

respectively.

For notational convenience, let U and V denote $\sum_{j=1}^{N_B}\left|h_{gB_j}\right|^2$ and $\sum_{j=1}^{N_B}\left|h_{iB_j}\right|^2$, respectively. Similarly to (C.1), T_{2_0} can be formulated as

$$\begin{aligned} T_{2\_0} &= \int_0^\infty \prod_{g\in D,g\neq i}\left(1-\exp\left(-\frac{v}{\lambda_{gj}}\right)\sum_{l=0}^{N_B-1}\frac{1}{l!}\left(\frac{v}{\lambda_{gj}}\right)^l\right) \frac{1}{\lambda_{ij}^{N_B}\left(N_B-1\right)!}v^{N_B-1}\exp\left(-\frac{v}{\lambda_{ij}}\right)dv \\ &= \sum_{S'}\frac{\beta_1\left(\beta_2+N_B-1\right)!}{\lambda_{ij}^{N_B}\left(N_B-1\right)!}\left(\frac{1}{\lambda_{ij}}+\beta_3\right)^{-\beta_2-N_B}. \end{aligned} \quad \text{(E.3)}$$

Using (E.3), (B.6) and (B.7), T_2 and T_3 can be obtained as

$$T_2=\sum_{S'}\frac{\beta_1\left(\beta_2+N_B-1\right)!}{\lambda_{ij}^{N_B}\left(N_B-1\right)!}\left(\frac{1}{\lambda_{ij}}+\beta_3\right)^{-\beta_2-N_B}I_2 \quad \text{(E.4)}$$

and

$$T_3=\sum_{S'}\frac{\beta_1\left(\beta_2+N_B-1\right)!}{\lambda_{ij}^{N_B}\left(N_B-1\right)!}\left(\frac{1}{\lambda_{ij}}+\beta_3\right)^{-\beta_2-N_B}I_3, \quad \text{(E.5)}$$

respectively.

REFERENCES

[1] J. Ren, J. Hu, D. Zhang, H. Guo, Y. Zhang and X. Shen, "RF energy harvesting and transfer in cognitive radio sensor networks: Opportunities and challenges," *IEEE Commun. Mag.*, vol. 56, no. 1, pp. 104-110, Jan. 2018.

[2] A. Banerjee, A. Paul and S. P. Maity, "Joint power allocation and route selection for outage minimization in multihop cognitive radio networks with energy harvesting," *IEEE Trans. Cognitive Commun. and Netw.*, vol. 4, no. 1, pp. 82-92, Mar. 2018.

[3] R. Zhang and C. K. Ho, "MIMO broadcasting for simultaneous wireless information and power transfer," *IEEE Trans. Wireless Commun.*, vol. 12, no. 5, pp. 1989-2001, May 2013.

[4] Y. Liu, S. Mousavifar, Y. Deng, C. Leung and M. Elkashlan, "Wireless energy harvesting in a cognitive relay network," *IEEE Trans. Wireless Commun.*, vol. 15, no. 4, pp. 2498-2508, Apr. 2016.

[5] A. Al-Talabani, Y. Deng, A. Nallanathan and H. X. Nguyen, "Enhancing secrecy rate in cognitive radio networks via stackelberg game," *IEEE Trans. Commun.*, vol. 64, no. 11, pp. 4764-4775, Nov. 2016.

[6] A. D. Wyner, "The wire-tap channel," *Bell System Technical Journal*, vol. 54, no. 8, pp. 1355-1387, 1975.

[7] S. Leung-Yan-Cheong and M. Hellman, "The Gaussian wiretap channel," *IEEE Trans. Inf. Theory*, vol. 24, no. 4, pp. 451-456, Jul. 1978.

[8] X. Chen and Y. Zhang, "Mode selection in MU-MIMO downlink networks: A physical-layer security perspective," *IEEE Systems Journal*, vol. 11, no. 2, pp. 1128-1136, Jun. 2017.

[9] H. M. Wang, K. W. Huang, Q. Yang and Z. Han, "Joint source-relay secure precoding for MIMO relay networks with direct links," *IEEE Trans. Commun.*, vol. 65, no. 7, pp. 2781-2793, Jul. 2017.

[10] B. Wang, P. Mu and Z. Li, "Artificial-noise-aided beamforming design in the MISOME wiretap channel under the secrecy outage probability constraint," *IEEE Trans. Wireless Commun.*, vol. 16, no. 11, pp. 7207-7220, Nov. 2017.

[11] C. Jeong, I. Kim and K. Dong, "Joint secure beamforming design at the source and the relay for an amplify-and-forward MIMO untrusted relay system," *IEEE Trans. Signal Process.*, vol. 60, no. 1, pp. 310-325, Jan. 2012.

[12] Y. Liu, J. Li and A. Petropulu, "Destination assisted cooperative jamming for wireless physical-layer security," *IEEE Trans. Inf. Forensics Security*, vol. 8, no. 4, pp. 682-694, Apr. 2013.

[13] H. M. Wang, F. Liu and M. C. Yang, "Joint cooperative beamforming, jamming, and power allocation to secure AF relay systems," *IEEE Trans. Veh. Tech.*, vol. 64, no. 10, pp. 4893-4898, Oct. 2015.

[14] H. Deng, H. Wang, J. Yuan, W. Wang and Q. Yin, "Secure communication in uplink transmissions: User selection and multiuser secrecy gain," *IEEE Trans. Commun.*, vol. 64, no. 8, pp. 3492-3506, Aug. 2016.

[15] I. Bang, S. Kim and D. Sung, "Artificial noise-aided user scheduling for optimal secrecy multiuser diversity," *IEEE Commun. Lett.*, vol. 21, no. 3, pp. 528-531, Mar. 2017.

[16] S. Poursajadi and M. H. Madani, "Analysis and enhancement of joint security and reliability in cooperative networks," *IEEE Trans. Veh. Tech.*, vol. 67, no. 12, pp. 12003-12012, Dec. 2018.

[17] H. Deng, H. Wang, G. Wei and W. Wang, "Secrecy transmission with a helper: To relay or to jam," *IEEE Trans. Inf. Forensics Security*, vol. 10, no. 2, pp. 293-307, Feb. 2015.

[18] Z. Ding, M. Zheng and P. Fan, "Asymptotic studies for the impact of antenna selection on secure two-way relaying communications with artificial noise," *IEEE Trans. Wireless Commun.*, vol. 13, pp. 2189-2203, Apr. 2014.

[19] X. Ding, T. Song, Y. Zou, X. Chen and L. Hanzo, "Security-reliability tradeoff analysis of artificial noise aided two-way opportunistic relay selection," *IEEE Trans. Veh. Tech.*, vol. 66, no. 5, pp. 3930-3941, May 2017.

[20] Y. Wu and X. Chen, "Robust beamforming and power splitting for secrecy wireless information and power transfer in cognitive relay networks," *IEEE Commun. Lett.*, vol. 20, no. 6, pp. 1152-1155, Jun. 2016.

[21] X. Chen, L. Guo, X. Li, C. Dong, J. Lin and P. T. Mathiopoulos, "Secrecy rate optimization for cooperative cognitive radio networks aided by a wireless energy harvesting jammer," *IEEE Access*, vol. 6, pp. 34127-34134, 2018.

[22] F. Zhou, Z. Li, J. Cheng, Q. Li and J. Si, "Robust AN-aided beamforming and power splitting design for secure MISO cognitive radio with SWIPT," *IEEE Trans. Wireless Commun.*, vol. 16, no. 4, pp. 2450-2464, Apr. 2017.

[23] M. Li, H. Yin, Y. Huang, Y. Wang and R. Yu, "Physical layer security in overlay cognitive radio networks with energy harvesting," *IEEE Trans. Veh. Tech.*, vol. 67, no. 11, pp. 11274-11279, Nov. 2018.

[24] H. Lei, M. Xu, I. Ansari, G. Pan, K. Qaraqe and M. Alouini, "On secure underlay MIMO cognitive radio networks with energy harvesting and transmit antenna selection," *IEEE Trans. Green Commun. and Netw.*, vol. 1, no. 2, pp. 192-203, Jun. 2017.

[25] C. E. Shannon, "A mathematical theory of communication," *Bell Syst. Tech. J.*, vol. 27, pp. 379-423, Oct. 1948.

[26] Y. Zou, "Intelligent interference exploitation for heterogeneous cellular networks against eavesdropping," *IEEE J. Sel. Areas Commun.*, Early Access, 2018.

[27] X. Tang, R. Liu, P. Spasojevic and H. V. Poor, "On the throughput of secure hybrid-ARQ protocols for Gaussian block-fading channels," *IEEE Trans. Inf. Theory*, vol. 55, no. 4, pp. 1575-1591, Apr. 2009.

[28] Y. Zou, X. Li and Y. Liang, "Secrecy outage and diversity analysis of cognitive radio systems," *IEEE J. Sel. Areas Commun.*, vol. 32, no. 11, pp. 2222-2236, Nov. 2014.

[29] N. Yang, P. L. Yeoh, M. Elkashlan, R. Schober and I. B. Collings, "Transmit antenna selection for security enhancement in MIMO wiretap channels," *IEEE Trans. Commun.*, vol. 61, no. 1, pp. 144-154, Jan. 2013.
[30] H. Lei, H. Zhang, I. Ansari, C. Gao, Y. Guo, G. Pan and K. Qaraqe, "Secrecy outage performance for SIMO underlay cognitive radio systems with generalized selection combining over Nakagami-m channels," *IEEE Trans. Veh. Technol.*, vol. 65, no. 12, pp. 10126-10132, Dec. 2016.
[31] E. Boshkovska, D. W. K. Ng, N. Zlatanov and R. Schober, "Practical nonlinear energy harvesting model and resource allocation for SWIPT systems," *IEEE Commun. Lett.*, vol. 19, no. 12, pp. 2082-2085, Dec. 2015.
[32] Y. Dong, M. J. Hossain and J. Cheng, "Performance of wireless powered amplify and forward relaying over Nakagami-m fading channels with nonlinear energy harvester," *IEEE Commun. Lett.*, vol. 20, no. 4, pp. 672-675, Apr. 2016.
[33] X. Di, K. Xiong, P. Fan and H. Yang, "Simultaneous wireless information and power transfer in cooperative relay networks with rateless codes," *IEEE Trans. Veh. Technol.*, vol. 66, no. 4, pp. 2981-2996, Apr. 2017.
[34] L. Wang, F. Hu, Z. Ling and B. Wang, "Wireless information and power transfer to maximize information throughput in WBAN," *IEEE Internet Things J.*, vol. 4, no. 5, pp. 1663-1670, Oct. 2017.
[35] K. Xiong, C. Chen, G. Qu, P. Fan and K. B. Letaief, "Group cooperation with optimal resource allocation in wireless powered communication networks," *IEEE Trans. Wireless Commun.*, vol. 16, no. 6, pp. 3840-3853, Jun. 2017.
[36] Z. Chen, L. Hadley, Z. Ding and X. Dai, "Improving secrecy performance of a wirelessly powered network," *IEEE Trans. Commun.*, vol. 65, no. 11, pp. 4996-5008, Nov. 2017.
[37] H. Al-Hraishawi and G. A. Aruma Baduge, "Wireless energy harvesting in cognitive massive MIMO systems with underlay spectrum sharing," *IEEE Wireless Commun. Lett.*, vol. 6, no. 1, pp. 134-137, Feb. 2017.
[38] D. W. K. Ng, E. S. Lo and R. Schober, "Multiobjective resource allocation for secure communication in cognitive radio networks with wireless information and power transfer," *IEEE Trans. Veh. Technol.*, vol. 65, no. 5, pp. 3166-3184, May 2016.
[39] X. Zhang, Y. Wang, F. Zhou, N. Al-Dhahir and X. Deng, "Robust resource allocation for MISO cognitive radio networks under two practical non-linear energy harvesting models," *IEEE Commun. Lett.*, vol. 22, no. 9, pp. 1874-1877, Sept. 2018.
[40] A. Jeffrey and D. Zwillinger, *Tables of intergrals, series, and products*, Sixth Edition, Elsevier, 2000.
[41] Y. Zou, X. Jiang, J. Zhu, Y. Ma, H. Gao, and C. Zhu, "Joint power splitting and relay selection for cooperative energy-harvesting communications," available online: https://arxiv.org/abs/1901.03301.

Xiaojin Ding received the Ph.D. degree in information and communication engineering from National Mobile Communication Research Laboratory, Southeast University (SEU), Nanjing, China. He is currently a Lecturer in Nanjing University of Posts and Telecommunications (NUPT), Nanjing, China. His research interests include space information network, cooperative communications, and physical-layer security.

Yulong Zou (SM'13) is a Full Professor and Doctoral Supervisor at the Nanjing University of Posts and Telecommunications (NUPT), Nanjing, China. He received the B.Eng. degree in information engineering from NUPT, Nanjing, China, in July 2006, the first Ph.D. degree in electrical engineering from the Stevens Institute of Technology, New Jersey, USA, in May 2012, and the second Ph.D. degree in signal and information processing from NUPT, Nanjing, China, in July 2012. His research interests span a wide range of topics in wireless communications and signal processing, including the cooperative communications, cognitive radio, wireless security, and energy-efficient communications. Dr. Zou was awarded the 9th IEEE Communications Society Asia-Pacific Best Young Researcher in 2014 and a co-receipt of the Best Paper Award at the 80th IEEE Vehicular Technology Conference in 2014. He is currently serving as an editor for the IEEE Communications Surveys & Tutorials, IET Communications, and China Communications. In addition, he has acted as TPC members for various IEEE sponsored conferences, e.g., IEEE ICC/GLOBECOM/WCNC/VTC/ICCC, etc.

Gengxin Zhang received his Bachelor, Master and Ph.D Degree in 1987, 1990 and 1994 respectively, all from Department of Radio Communication Engineering,Nanjing Institute of Communication Engineering, Nanjing, China. He is currently a Professor in Nanjing University of Posts and Telecommunications (NUPT), Nanjing, China. His research interests include the satellite communications, deep space communications and space information network, and is heading several projects in these areas.

Xiaoshu Chen is a Full Professor at the Southeast University (SEU), Nanjing, China. He received the M.S. degree in information engineering from SEU. His general research interests include communications theory and vehicle area network.

Xiaojun Wang is a Professor of National Mobile Communication Research Laboratory at Southeast University (SEU), Nanjing, China. He received his BS, MS and PhD degree in communication and information systems from SEU in 1996, 1999 and 2010, respectively. His research interests are in the areas of wireless networks and mobile communications.

Lajos Hanzo (http://www-mobile.ecs.soton.ac.uk) FREng, F'04, FIET, Fellow of EURASIP, received his 5-year degree in electronics in 1976 and his doctorate in 1983 from the Technical University of Budapest. In 2009 he was awarded an honorary doctorate by the Technical University of Budapest and in 2015 by the University of Edinburgh. In 2016 he was admitted to the Hungarian Academy of Science. During his 40-year career in telecommunications he has held various research and academic posts in Hungary, Germany and the UK. Since 1986 he has been with the School of Electronics and Computer Science, University of Southampton, UK, where he holds the chair in telecommunications. He has successfully supervised 119 PhD students, co-authored 18 John Wiley/IEEE Press books on mobile radio communications totalling in excess of 10 000 pages, published 1800+ research contributions at IEEE Xplore, acted both as TPC and General Chair of IEEE conferences, presented keynote lectures and has been awarded a number of distinctions. Currently he is directing a 60-strong academic research team, working on a range of research projects in the field of wireless multimedia communications sponsored by industry, the Engineering and Physical Sciences Research Council (EPSRC) UK, the European Research Council's Advanced Fellow Grant and the Royal Society's Wolfson Research Merit Award. He is an enthusiastic supporter of industrial and academic liaison and he offers a range of industrial courses. He is also a Governor of the IEEE ComSoc and VTS. He is a former Editor-in-Chief of the IEEE Press and a former Chaired Professor also at Tsinghua University, Beijing. For further information on research in progress and associated publications please refer to http://www-mobile.ecs.soton.ac.uk